Communications in Applied Mathematics and Computational Science

A NUMERICAL STUDY OF THE EXTENDED KOHN–SHAM GROUND STATES OF ATOMS

ERIC CANCÈS AND NAHIA MOURAD

vol. 13 no. 2 2018

msp

COMM. APP. MATH. AND COMP. SCI.
Vol. 13, No. 2, 2018
dx.doi.org/10.2140/camcos.2018.13.139

A NUMERICAL STUDY OF THE EXTENDED KOHN–SHAM GROUND STATES OF ATOMS

ERIC CANCÈS AND NAHIA MOURAD

In this article, we consider the extended Kohn–Sham model for atoms subjected to cylindrically symmetric external potentials. The variational approximation of the model and the construction of appropriate discretization spaces are detailed together with the algorithm to solve the discretized Kohn–Sham equations used in our code. Using this code, we compute the occupied and unoccupied energy levels of all the atoms of the first four rows of the periodic table for the reduced Hartree–Fock (rHF) and the extended Kohn–Sham Xα models. These results allow us to test numerically the assumptions on the negative spectra of atomic rHF and Kohn–Sham Hamiltonians used in our previous theoretical works on density functional perturbation theory and pseudopotentials. Interestingly, we observe accidental degeneracies between s and d shells or between p and d shells at the Fermi level of some atoms. We also consider the case of an atom subjected to a uniform electric field. For various magnitudes of the electric field, we compute the response of the density of the carbon atom confined in a large ball with Dirichlet boundary conditions, and we check that, in the limit of small electric fields, the results agree with the ones obtained with first-order density functional perturbation theory.

1. Introduction

Since the introduction by Dirac in 1929 of a many-body nonrelativistic quantum Hamiltonian allowing a comprehensive description of the physical and chemical properties of atoms and molecules [12], countless research articles and several monographs [2; 11; 16; 17; 28; 38; 39] have been devoted to the calculation of the ground states of atoms. Some of these works aimed at computing numerically the atomic ground state energy of the helium atom — the simplest nontrivial case — with spectroscopic accuracy using relativistic corrections to Dirac's nonrelativistic model [21]. On the other extremity of the spectrum, other works focused on proving mathematical theorems about the asymptotic limit of the nonrelativistic [25; 33; 14] or relativistic [36] ground state energy and density of neutral atoms when the

MSC2010: 35P30, 35Q40, 65Z05, 81V45.
Keywords: density functional theory, electronic structure of atoms, extended Kohn–Sham model, Stark effect.

nuclear charge goes to infinity. The mathematical foundation of Hund's rule, the well known empirical recipe to fill in the occupied spin orbitals of atoms, was elucidated in the limit of weak electronic interactions [15]. Interesting articles containing new results on atomic electronic structures in the framework of density functional theory have been recently published [22; 26].

This work is concerned with extended Kohn–Sham models for atoms. Recall that extended Kohn–Sham models are (zero-temperature) Kohn–Sham models allowing fractional occupancies of the Kohn–Sham orbitals (see [13] and references therein). The exact extended Kohn–Sham model, that is, the extended Kohn–Sham model with exact exchange-correlation functional, is obtained by applying Levy's constraint search method [23] to the mixed-state variational formulation of the electronic ground-state problem [40]. Alternatively, the exact extended Kohn–Sham density functional can be seen as the Legendre–Fenchel transform of the functional mapping external potentials onto electronic ground-state energies [24]. Among other interesting mathematical features, the exact extended Kohn–Sham model is convex in the density, which is not the case of the standard Kohn–Sham model.

The simplest instance of extended Kohn–Sham model is the reduced Hartree–Fock (rHF, also called Hartree) model [35]. It is obtained by setting to zero the exchange-correlation energy functional. Although this model is too crude to obtain accurate properties of atoms and molecules, it is extremely interesting from a mathematical point of view, since its structure is very similar to the Kohn–Sham models actually used in chemistry and physics, while being *strictly convex* in the density. As a result, the rHF ground state density of a given molecular system, if it exists, is unique, and shares the symmetry properties of the nuclear distribution. In particular, the rHF density of any neutral atom is unique and spherically symmetric. Uniqueness of the ground-state density is also key to rigorously establish mathematical results in the thermodynamic limit for perfect crystals [10], crystals with points defects [3], or disordered materials [4]. The rHF model therefore is of particular interest for mathematicians. One of the motivations of the present work is to contribute to a better understanding of the rHF model, by carefully investigating the structures of rHF atomic ground states. We will also consider extended Kohn–Sham LDA (local density approximation) models [20; 29]. We will study the case of an isolated atom, as well as the case of an atom subjected to cylindrically symmetric external potential. We notably have in mind Stark potentials, which are potentials of the form $W(\boldsymbol{r}) = -\mathscr{E} \cdot \boldsymbol{r}$ generated by a uniform electric field $\mathscr{E} \neq 0$.

We first propose a method to accurately solve the extended Kohn–Sham problem for cylindrically symmetric systems, using spherical coordinates and a separation of variables. This approach is based on the fact that, for such systems, the Kohn–Sham Hamiltonian commutes with L_z, the z-component of the angular momentum

operator, z denoting the symmetry axis of the system. We obtain in this way a family of 2D elliptic eigenvalue problems in the r and θ variables, indexed by the eigenvalue $m \in \mathbb{Z}$ of L_z, all these problems being coupled together through the self-consistent density. To discretize the 2D eigenvalue problems, we use harmonic polynomials in θ (or in other words, spherical harmonics Y_l^0, which only depend on θ) to discretize along the angular variable, and high-order finite element methods to discretize along the radial variable $r \in [0, L_e]$. We then apply this approach to study numerically two kinds of systems.

First, we provide accurate approximations of the extended Kohn–Sham ground states of all the atoms of the first four rows of the periodic table. These results allow us to test numerically the assumptions on the negative spectra of atomic rHF and Kohn–Sham LDA Hamiltonians that we used in previous theoretical works on density functional perturbation theory [7] and norm-conserving semilocal pseudopotentials [8]. We show in particular that for most atoms of the first four rows of the periodic table, the Fermi level is negative and is not an accidentally degenerate eigenvalue of the rHF Hamiltonian. We also observe that there seems to be no unoccupied orbitals with negative energies. On the other hand, for some chemical elements, the Fermi level seems to be an accidentally degenerate eigenvalue (for example the rHF 5s and 4d states of the palladium atom seem to be degenerate). For a few of them, this accidentally degenerate eigenvalue is so close to zero that our calculations do not allow us to know whether it is slightly negative or equal to zero. For instance, our simulations seem to show that the 5s and 3d states of the iron atom seem to be degenerate at the rHF level of theory, and the numerical value of their energy we obtain with our code is about -10^{-5} Ha.

Second, we study an atom subjected to a uniform electric field (Stark effect). In this case, the system has no ground state (the Kohn–Sham energy functional is not bounded below), but density functional perturbation theory (see [7; 8] for a mathematical analysis) can be used to compute the polarization of the electronic cloud caused by the external electric field. The polarized electronic state is not a steady state, but a resonant state, and the smaller the electric field, the longer its life time. Another way to compute the polarization of the electronic cloud is to compute the ground state for a small enough electric field in a basis set consisting of functions decaying fast enough at infinity for the electrons to stay close to the nuclei. The Gaussian basis functions commonly used in quantum chemistry satisfy this decay property. However, it is not easy to obtain very accurate results with Gaussian basis sets, since they are not systematically improvable (over-completeness issues). Here we consider instead basis functions supported in a ball B_{L_e}, where L_e is a numerical parameter chosen large enough to obtain accurate results and small enough to prevent electrons from escaping to infinity (for a given, small, value of the external electric field $\mathscr{E}$). We study the ground state energy and density

as functions of the cut-off radius L_e, and observe that for a given, small enough, uniform electric field, there is a plateau $[L_{e,\min}, L_{e,\max}]$ on which these quantities hardly vary. For $L_e < L_{e,\min}$, the simulated system is too much confined, which artificially increases its energy, while for $L_e > L_{e,\max}$, a noticeable amount of charge accumulates at the boundary of the simulation domain, in the direction of $\mathscr{E}$ (where the potential energy is very negative). On the other hand, for $L_{e,\min} \le L_e \le L_{e,\max}$, the simulation provides a fairly accurate approximation of the polarization energy and the polarized density.

The article is organized as follows. In Section 2, we recall the mathematical formulation of the extended Kohn–Sham model, and some theoretical results about the rHF and LDA ground states of isolated atoms and of atoms subjected to an external cylindrically symmetric potential. In Section 3, we describe the discretization method and the algorithms used in this work to compute the extended Kohn–Sham ground states of atoms subjected to cylindrically symmetric external potentials. Some numerical results are presented in Section 4.

2. Modeling

In this article, we consider a molecular system consisting of a single nucleus of atomic charge $Z \in \mathbb{N}^*$ and of N electrons. For $N = Z$, this system is the neutral atom with nuclear charge Z, which we call atom Z for convenience.

2.1. ***Kohn–Sham models for atoms.*** In the framework of the (extended) Kohn–Sham model [13], the ground state energy of a system with one nucleus with charge Z and N electrons is obtained by minimizing an energy functional of the form

$$E_{Z,N}(\gamma) := \mathrm{Tr}(-\tfrac{1}{2}\Delta\gamma) - Z\int_{\mathbb{R}^3} \frac{\rho_\gamma}{|\cdot|} + \tfrac{1}{2}D(\rho_\gamma, \rho_\gamma) + E_{\mathrm{xc}}(\rho_\gamma) \tag{1}$$

over the set

$$\mathscr{K}_N := \{\gamma \in \mathscr{S}(L^2(\mathbb{R}^3)) \mid 0 \le \gamma \le 2,\ \mathrm{Tr}(\gamma) = N,\ \mathrm{Tr}(-\Delta\gamma) < \infty\}, \tag{2}$$

where $\mathscr{S}(L^2(\mathbb{R}^3))$ is the space of the self-adjoint operators on $L^2(\mathbb{R}^3) := L^2(\mathbb{R}^3, \mathbb{R})$ and $\mathrm{Tr}(-\Delta\gamma) := \mathrm{Tr}(|\nabla|\gamma|\nabla|)$. Note that $\mathscr{K}_N$ is a closed convex subset of the space $\mathfrak{S}_{1,1}$ defined by

$$\mathfrak{S}_{1,1} := \{T \in \mathfrak{S}_1 \mid |\nabla|T|\nabla| \in \mathfrak{S}_1\},$$

endowed with norm

$$\|T\|_{\mathfrak{S}_{1,1}} := \|T\|_{\mathfrak{S}_1} + \||\nabla|T|\nabla|\|_{\mathfrak{S}_1}.$$

The function $-Z/|\cdot|$ is the attraction potential induced on the electrons by the nucleus, and ρ_γ is the density associated with the one-body density matrix γ. For

$\gamma \in \mathcal{K}_N$, we have

$$\rho_\gamma \geq 0, \quad \int_{\mathbb{R}^3} \rho_\gamma = N, \quad \int_{\mathbb{R}^3} |\nabla \sqrt{\rho_\gamma}|^2 \leq \mathrm{Tr}(-\Delta\gamma) < \infty.$$

The last result is the Hoffmann-Ostenhof inequality [19]. Therefore, we have

$$\sqrt{\rho_\gamma} \in H^1(\mathbb{R}^3),$$

and in particular,

$$\rho_\gamma \in L^1(\mathbb{R}^3) \cap L^3(\mathbb{R}^3).$$

For $\rho \in L^{6/5}(\mathbb{R}^3)$, $D(\rho, \rho)$ is equal to $\int_{\mathbb{R}^3} V^{\mathrm{H}}(\rho)\rho$, where V^{H} is the Coulomb, also called Hartree, potential generated by ρ:

$$V^{\mathrm{H}}(\rho) = \rho \star |\cdot|^{-1}.$$

Recall that V^{H} can be seen as a unitary operator from the Coulomb space $\mathcal{C}$ to its dual $\mathcal{C}'$, where

$$\mathcal{C} := \{\rho \in \mathcal{S}'(\mathbb{R}^3) \mid \hat{\rho} \in L^1_{\mathrm{loc}}(\mathbb{R}^3, \mathbb{C}),\ |\cdot|^{-1}\hat{\rho} \in L^2(\mathbb{R}^3, \mathbb{C})\},$$
$$(\rho_1, \rho_2)_{\mathcal{C}} = 4\pi \int_{\mathbb{R}^3} \frac{\hat{\rho}_1(\boldsymbol{k})^* \hat{\rho}_2(\boldsymbol{k})}{|\boldsymbol{k}|^2}\, d\boldsymbol{k}, \quad (3)$$

and

$$\mathcal{C}' := \{v \in L^6(\mathbb{R}^3) \mid \nabla v \in (L^2(\mathbb{R}^3))^3\},$$
$$(v_1, v_2)_{\mathcal{C}'} = \frac{1}{4\pi} \int_{\mathbb{R}^3} \nabla v_1 \nabla v_2 = \frac{1}{4\pi} \int_{\mathbb{R}^3} |\boldsymbol{k}|^2 \hat{v}_1(\boldsymbol{k})^* \hat{v}_2(\boldsymbol{k})\, d\boldsymbol{k}. \quad (4)$$

The term E_{xc} is the exchange-correlation energy. We will restrict ourselves to two kinds of Kohn–Sham models: the rHF model, for which the exchange-correlation energy is taken equal to zero,

$$E_{\mathrm{xc}}^{\mathrm{rHF}} = 0,$$

and the Kohn–Sham LDA (local density approximation) model, for which the exchange-correlation energy has the form

$$E_{\mathrm{xc}}^{\mathrm{LDA}}(\rho) = \int_{\mathbb{R}^3} \epsilon_{\mathrm{xc}}(\rho(r))\, dr,$$

where ϵ_{xc} is the sum of the exchange and correlation energy densities of the homogeneous electron gas. As the function $\epsilon_{\mathrm{xc}} : \mathbb{R}_+ \to \mathbb{R}$ is not explicitly known, it is approximated in practice by an explicit function, still denoted by ϵ_{xc} for simplicity. We assume here that the approximate function ϵ_{xc} is a C^1 function from $\mathbb{R}_+$ into $\mathbb{R}_-$,

twice differentiable on $\mathbb{R}_+^*$, and obeying the conditions

$$\epsilon_{\mathrm{xc}}(0) = 0, \qquad \epsilon'_{\mathrm{xc}}(0) \le 0, \tag{5}$$

$$\text{there exists } 0 < \beta_- \le \beta_+ < \tfrac{2}{3} \quad \text{such that } \sup_{\rho \in \mathbb{R}_+} \frac{|\epsilon'_{\mathrm{xc}}(\rho)|}{\rho^{\beta_-} + \rho^{\beta_+}} < \infty, \tag{6}$$

$$\text{there exists } 1 \le \alpha < \tfrac{3}{2} \quad \text{such that } \limsup_{\rho \to 0_+} \frac{\epsilon_{\mathrm{xc}}(\rho)}{\rho^{\alpha}} < 0, \tag{7}$$

$$\text{there exists } \lambda > -1 \quad \text{such that } \epsilon''_{\mathrm{xc}}(\rho) \underset{\rho \to 0_+}{\sim} c\rho^{\lambda}. \tag{8}$$

Note that these properties are satisfied by the exact function ϵ_{xc}. They are also satisfied by Slater's Xα model for which $\epsilon_{\mathrm{xc}}(\rho) = -C_{\mathrm{D}}\rho^{1/3}$, where $C_{\mathrm{D}} = \frac{3}{4}(\frac{3}{\pi})^{1/3}$ is the Dirac constant. This model is used in the simulations reported in Section 4.

Remark. The minimization set $\mathcal{K}_N$ defined in (2) is the set of *real spin-unpolarized* first-order reduced density matrices. We will call its elements *nonmagnetic states*. The general (complex noncollinear spin-polarized; see, e.g., [18]) rHF model being convex in the density matrix, and strictly convex in the density, the general rHF ground state density of a given molecular system in the absence of magnetic field, if it exists, is unique, and one of the minimizers is a nonmagnetic state. Indeed, using the notation of [18], if γ is a complex noncollinear spin-polarized ground state, the nonmagnetic state

$$\gamma_0 := \tfrac{1}{4}(\gamma^{\uparrow\uparrow} + \overline{\gamma^{\uparrow\uparrow}} + \gamma^{\downarrow\downarrow} + \overline{\gamma^{\downarrow\downarrow}}),$$

where $\overline{\gamma^{\sigma,\sigma}}$ is the complex conjugate (not the adjoint) of the operator $\gamma^{\sigma,\sigma}$, is a nonmagnetic ground state. The general rHF ground state energy and density of a molecular system in the absence of magnetic field can therefore be determined by minimizing the rHF energy functional over the set $\mathcal{K}_N$. The LDA model is not a priori strictly convex in the density, but it is convex over the set of complex noncollinear spin-polarized density matrices having a given density ρ. Therefore, the general LDA ground state energy and densities can be obtained by minimizing the LDA energy functional over the set $\mathcal{K}_N$. In contrast, this argument does not apply to the local spin density approximation (LSDA) model, whose ground states are, in general, spin-polarized.

To avoid ambiguity, for any Z and N in $\mathbb{R}_+^*$, we denote

$$\mathcal{I}_{Z,N}^{\mathrm{rHF}} := \inf\{E_{Z,N}^{\mathrm{rHF}}(\gamma) \mid \gamma \in \mathcal{K}_N\}, \tag{9}$$

where

$$E_{Z,N}^{\mathrm{rHF}}(\gamma) := \mathrm{Tr}(-\tfrac{1}{2}\Delta\gamma) - Z\int_{\mathbb{R}^3} \frac{\rho_\gamma}{|\cdot|} + \tfrac{1}{2}D(\rho_\gamma, \rho_\gamma),$$

and

$$\mathcal{I}_{Z,N}^{\mathrm{LDA}} := \inf\{E_{Z,N}^{\mathrm{LDA}}(\gamma) \mid \gamma \in \mathcal{K}_N\}, \tag{10}$$

where

$$E^{\mathrm{LDA}}_{Z,N}(\gamma) := \mathrm{Tr}(-\tfrac{1}{2}\Delta\gamma) - Z\int_{\mathbb{R}^3}\frac{\rho_\gamma}{|\cdot|} + \tfrac{1}{2}D(\rho_\gamma,\rho_\gamma) + E^{\mathrm{LDA}}_{\mathrm{xc}}(\rho_\gamma).$$

We recall the following two theorems which ensure the existence of ground states for neutral atoms and positive ions.

Theorem 1 (ground state for the rHF model [7; 35]). *Let $Z \in \mathbb{R}^*_+$ and $N \le Z$. Then the minimization problem* (9) *has a ground state $\gamma^{0,\mathrm{rHF}}_{Z,N}$, and all the ground states share the same density $\rho^{0,\mathrm{rHF}}_{Z,N}$. The mean-field Hamiltonian*

$$H^{0,\mathrm{rHF}}_{Z,N} := -\tfrac{1}{2}\Delta - \frac{Z}{|\cdot|} + V^{\mathrm{H}}(\rho^{0,\mathrm{rHF}}_{Z,N})$$

is a bounded-below self-adjoint operator on $L^2(\mathbb{R}^3)$, $\sigma_{\mathrm{ess}}(H^{0,\mathrm{rHF}}_{Z,N}) = \mathbb{R}_+$, and the ground state $\gamma^{0,\mathrm{rHF}}_{Z,N}$ is of the form

$$\gamma^{0,\mathrm{rHF}}_{Z,N} = 2\mathbb{1}_{(-\infty,\epsilon^{0,\mathrm{rHF}}_{Z,N,\mathrm{F}})}(H^{0,\mathrm{rHF}}_{Z,N}) + \delta^{0,\mathrm{rHF}}_{Z,N},$$

where $\epsilon^{0,\mathrm{rHF}}_{Z,N,\mathrm{F}} \le 0$ is the Fermi level, $\mathrm{Ran}(\delta^{0,\mathrm{rHF}}_{Z,N}) \subset \mathrm{Ker}(H^{0,\mathrm{rHF}}_{Z,N} - \epsilon^{0,\mathrm{rHF}}_{Z,N,\mathrm{F}})$, *and $0 \le \delta^{0,\mathrm{rHF}}_{Z,N} \le 2$. If $\epsilon^{0,\mathrm{rHF}}_{Z,N,\mathrm{F}}$ is negative and is not an accidentally degenerate eigenvalue of $H^{0,\mathrm{rHF}}_{Z,N}$, then the nonmagnetic ground state $\gamma^{0,\mathrm{rHF}}_{Z,N}$ is unique.*

Our numerical results indicate that, for neutral atoms, the assumption

$$\epsilon^{0,\mathrm{rHF}}_{Z,Z,\mathrm{F}} \text{ is negative and is not an accidentally degenerate eigenvalue of } H^{0,\mathrm{rHF}}_{Z,Z}$$

is satisfied for most chemical elements of the first four rows, but not for all of them. We will elaborate on this observation in Section 4.1.1.

Theorem 2 (ground state for the LDA model [1]). *Let $Z \in \mathbb{R}^*_+$ and $N \le Z$. Suppose that* (5)–(7) *hold. Then the minimization problem* (10) *has a ground state $\gamma^{0,\mathrm{LDA}}_{Z,N}$. In addition, $\gamma^{0,\mathrm{LDA}}_{Z,N}$ satisfies the self-consistent field equation*

$$\gamma^{0,\mathrm{LDA}}_{Z,N} = 2\mathbb{1}_{(-\infty,\epsilon^{0,\mathrm{LDA}}_{Z,N,\mathrm{F}})}(H^{0,\mathrm{LDA}}_{Z,N}) + \delta^{0,\mathrm{LDA}}_{Z,N}, \tag{11}$$

where $\epsilon^{0,\mathrm{LDA}}_{Z,N,\mathrm{F}} \le 0$ is the Fermi level, $\mathrm{Ran}(\delta^{0,\mathrm{LDA}}_{Z,N}) \subset \mathrm{Ker}(H^{0,\mathrm{LDA}}_{Z,N} - \epsilon^{0,\mathrm{LDA}}_{Z,N,\mathrm{F}})$, $0 \le \delta^{0,\mathrm{LDA}}_{Z,N} \le 2$, *and the mean-field Hamiltonian*

$$H^{0,\mathrm{LDA}}_{Z,N} := -\tfrac{1}{2}\Delta - \frac{Z}{|\cdot|} + V^{\mathrm{H}}(\rho^{0,\mathrm{LDA}}_{Z,N}) + v_{\mathrm{xc}}(\rho^{0,\mathrm{LDA}}_{Z,N}),$$

where $\rho^{0,\mathrm{LDA}}_{Z,N} = \rho_{\gamma^{0,\mathrm{LDA}}_{Z,N}}$ and $v_{\mathrm{xc}}(\rho) = \frac{d\epsilon_{\mathrm{xc}}}{d\rho}(\rho)$, is a bounded-below self-adjoint operator on $L^2(\mathbb{R}^3)$ and $\sigma_{\mathrm{ess}}(H^{0,\mathrm{LDA}}_{Z,N}) = \mathbb{R}_+$.

2.2. ***Density functional perturbation theory.*** We now examine the response of the ground state density matrix when an additional external potential βW is turned on. The energy functional to be minimized over $\mathcal{K}_N$ now reads

$$\widetilde{E}^{\mathrm{rHF/LDA}}_{Z,N}(\gamma, \beta W) := E^{\mathrm{rHF/LDA}}_{Z,N}(\gamma) + \int_{\mathbb{R}^3} \beta W \rho_\gamma, \tag{12}$$

and is well defined for any $\gamma \in \mathcal{K}_N$, $W \in \mathscr{C}'$, and $\beta \in \mathbb{R}$. The parameter β is called the coupling constant in quantum mechanics. Denote by

$$\widetilde{\mathcal{I}}^{\mathrm{rHF/LDA}}_{Z,N}(\beta W) := \inf\{\widetilde{E}^{\mathrm{rHF/LDA}}_{Z,N}(\gamma, \beta W) \mid \gamma \in \mathcal{K}_N\}. \tag{13}$$

The following theorem ensures the existence of a perturbed ground state density matrix for perturbation potentials in $\mathscr{C}'$.

Theorem 3 (existence of a perturbed minimizer [7]). *Let $Z \in \mathbb{R}^*_+$, $N \leq Z$, and $W \in \mathscr{C}'$. Assume that the Fermi level $\epsilon^{0,\mathrm{rHF}}_{Z,N,\mathrm{F}}$ is negative and is not an accidentally degenerate eigenvalue of $H^{0,\mathrm{rHF}}_{Z,N}$. Then the nonmagnetic unperturbed rHF ground state, that is, the minimizer of* (9), *is unique, and the perturbed problem* (13) *has a unique nonmagnetic ground state $\gamma^{\mathrm{rHF}}_{Z,N,\beta W}$, for $\beta \in \mathbb{R}$ small enough. The Hamiltonian*

$$H^{\mathrm{rHF}}_{Z,N,\beta W} = -\tfrac{1}{2}\Delta - \frac{Z}{|\cdot|} + V^{\mathrm{H}}(\rho^{\mathrm{rHF}}_{Z,N,\beta W}) + \beta W, \tag{14}$$

where $\rho^{\mathrm{rHF}}_{Z,N,\beta W} = \rho_{\gamma^{\mathrm{rHF}}_{Z,N,\beta W}}$, is a bounded-below self-adjoint operator on $L^2(\mathbb{R}^3)$ with form domain $H^1(\mathbb{R}^3)$ and $\sigma_{\mathrm{ess}}(H^{0,\mathrm{rHF}}_{Z,N,\beta W}) = \mathbb{R}_+$. Moreover, $\gamma^{\mathrm{rHF}}_{Z,N,\beta W}$ and $\rho^{\mathrm{rHF}}_{Z,N,\beta W}$ are analytic in β; that is,

$$\gamma^{\mathrm{rHF}}_{Z,N,\beta W} = \sum_{k\geq 0} \beta^k \gamma^{(k),\mathrm{rHF}}_{Z,N,W} \quad \textit{and} \quad \rho^{\mathrm{rHF}}_{Z,N,\beta W} = \sum_{k\geq 0} \beta^k \rho^{(k),\mathrm{rHF}}_{Z,N,W},$$

the above series being normally convergent in $\mathfrak{S}_{1,1}$ and $\mathscr{C}$, respectively.

In the sequel, we will refer to $\gamma^{(k)}_{Z,N,W}$ as the k-th-order perturbation of the density matrix.

Although we focus here on nonmagnetic states, it is convenient to consider $H^{0,\mathrm{rHF}}_{Z,N}$ as an operator on $L^2(\mathbb{R}^3, \mathbb{C})$ in order to expand the angular part of the atomic orbitals on the usual complex spherical harmonics. It would of course have been possible to avoid considering complex wave functions by expanding on real spherical harmonics. However, we have chosen to work with complex wave functions to prepare for future works on magnetic systems.

The unperturbed Hamiltonian $H^{0,\mathrm{rHF}}_{Z,N}$ is a self-adjoint operator on $L^2(\mathbb{R}^3, \mathbb{C})$ invariant with respect to rotations around the nucleus (assumed located at the origin). This operator is therefore block-diagonal in the decomposition of $L^2(\mathbb{R}^3, \mathbb{C})$ as the

direct sum of the pairwise orthogonal subspaces $\mathcal{H}_l := \mathrm{Ker}(\boldsymbol{L}^2 - l(l+1))$:

$$L^2(\mathbb{R}^3, \mathbb{C}) = \bigoplus_{l \in \mathbb{N}} \mathcal{H}_l,$$

where $\boldsymbol{L} = \boldsymbol{r} \times (-i\nabla)$ is the angular momentum operator. Since we are going to consider perturbation potentials which are not spherically symmetric, but only cylindrically symmetric, or in other words independent of the azimuthal angle φ in spherical coordinates, the $\mathcal{H}_l$ are no longer invariant subspaces of the perturbed Hamiltonians. The appropriate decomposition of $L^2(\mathbb{R}^3, \mathbb{C})$ into invariant subspaces for Hamiltonians $H^{\mathrm{rHF}}_{Z,N,\beta W}$ with W cylindrically symmetric is the following: for $m \in \mathbb{Z}$, we set

$$\mathcal{H}^m := \mathrm{Ker}(L_z - m),$$

where L_z is the z-component of the angular momentum operator $\boldsymbol{L}$ ($L_z = \boldsymbol{L} \cdot \boldsymbol{e}_z$).

Note that,

$$\text{for all } l \in \mathbb{N}, \quad \mathcal{H}_l = \left\{ \phi \in L^2(\mathbb{R}^3, \mathbb{C}) \;\middle|\; \phi(r, \theta, \varphi) = \sum_{-l \le m \le l} R^m(r) Y_l^m(\theta, \varphi) \right\},$$

and,

$$\text{for all } m \in \mathbb{Z}, \quad \mathcal{H}^m = \left\{ \phi \in L^2(\mathbb{R}^3, \mathbb{C}) \;\middle|\; \phi(r, \theta, \varphi) = \sum_{l \ge |m|} R_l(r) Y_l^m(\theta, \varphi) \right\},$$

where Y_l^m are the spherical harmonics, i.e., the joint eigenfunctions of Δ_S, the Laplace–Beltrami operator on the unit sphere $\mathbb{S}^2$ of $\mathbb{R}^3$, and $\mathcal{L}_z$ the generator of rotations about the azimuthal axis of $\mathbb{S}^2$. More precisely, we have

$$-\Delta_S Y_l^m = l(l+1) Y_l^m \quad \text{and} \quad \mathcal{L}_z Y_l^m = m Y_l^m,$$

where, in spherical coordinates,

$$\Delta_S = \frac{1}{\sin\theta} \frac{\partial}{\partial\theta} \left(\sin\theta \frac{\partial}{\partial\theta} \right) + \frac{1}{\sin^2\theta} \frac{\partial^2}{\partial\varphi^2} \quad \text{and} \quad \mathcal{L}_z = -i \frac{\partial}{\partial\varphi}.$$

These functions are orthonormal, in the sense that

$$\int_{\mathbb{S}^2} Y_l^m (Y_{l'}^{m'})^* = \int_{\theta=0}^{\pi} \int_{\varphi=0}^{2\pi} Y_l^m(\theta, \varphi) (Y_{l'}^{m'}(\theta, \varphi))^* \sin\theta \, d\theta \, d\varphi = \delta_{ll'} \delta_{mm'}, \tag{15}$$

where δ_{ij} is the Kronecker symbol and $(Y_l^m)^* = (-1)^m Y_l^{-m}$ is the complex conjugate of Y_l^m.

We also define

$$\mathcal{V}^m := \mathcal{H}^m \cap H^1(\mathbb{R}^3, \mathbb{C}),$$

so that $L^2(\mathbb{R}^3, \mathbb{C})$ and $H^1(\mathbb{R}^3, \mathbb{C})$ are decomposed as the direct sums

$$L^2(\mathbb{R}^3, \mathbb{C}) = \bigoplus_{m\in\mathbb{Z}} \mathcal{H}^m \quad \text{and} \quad H^1(\mathbb{R}^3, \mathbb{C}) = \bigoplus_{m\in\mathbb{Z}} \mathcal{V}^m, \tag{16}$$

each $\mathcal{H}^m$ being $H^{\mathrm{rHF}}_{Z,N,\beta W}$-stable (in the sense of unbounded operators) for W cylindrically symmetric. This is due to the fact that, for W cylindrically symmetric, the operator $H^{\mathrm{rHF}}_{Z,N,\beta W}$ commutes with L_z. Note that $\sigma(H^{\mathrm{rHF}}_{Z,N,\beta W}) = \overline{\bigcup_{m\in\mathbb{Z}} \sigma(H^{\mathrm{rHF}}_{Z,N,\beta W}|_{\mathcal{H}^m})}$. Same arguments hold true for $H^{\mathrm{LDA}}_{Z,N,\beta W}$ under the assumption that the ground state density $\rho^{0,\mathrm{LDA}}_{Z,N,\beta W}$ is cylindrically symmetric (which is the case whenever it is unique).

We are interested in the Stark potential

$$W_{\mathrm{Stark}}(\boldsymbol{r}) = -e_z \cdot \boldsymbol{r}, \tag{17}$$

which does not belong to $\mathcal{C}'$, and thus does not fall under the scope of Theorem 3. We therefore introduce the classes of perturbation potentials

$$\mathcal{W}_s := \left\{ W \in \mathcal{H}^0_{\mathrm{loc}} \;\middle|\; \int_{\mathbb{R}^3} \frac{|W(\boldsymbol{r})|^2}{(1+|\boldsymbol{r}|^2)^s}\, d\boldsymbol{r} < \infty \right\},$$

where $\mathcal{H}^0_{\mathrm{loc}} := \mathcal{H}^0 \cap L^2_{\mathrm{loc}}(\mathbb{R}^3)$, which contain the Stark potential W_{Stark} whenever $s > \frac{5}{2}$. For $W \in \mathcal{W}_s \setminus \mathcal{C}'$, the energy functional (12) is not necessarily bounded below on $\mathcal{K}_N$ for $\beta \neq 0$. Thus, the solution of (13) may not exist. This is the case for the Stark potential W_{Stark}. However, the k-th-order perturbation of the ground state may exist, as this is the case when the linear Schrödinger operator of the hydrogen atom is perturbed by the Stark potential W_{Stark} (see, e.g., [31]). The following theorem ensures the existence of the first-order perturbation of the density matrix.

Theorem 4 (first-order density functional perturbation theory [8]). *Let $Z \in \mathbb{R}^*_+$, $0 < N \leq Z$, such that $\epsilon^{0,\mathrm{rHF}}_{Z,N,\mathrm{F}}$ is negative*[1] *and is not an accidentally degenerate eigenvalue of $H^{0,\mathrm{rHF}}_{Z,N}$, $s \in \mathbb{R}$, and $W \in \mathcal{W}_s$. In the rHF framework, the first-order perturbation of the density matrix $\gamma^{(1),\mathrm{rHF}}_{Z,N,W}$ is well defined in $\mathfrak{S}_{1,1}$.*

Note that assumption (8) is used to establish the existence and uniqueness of the first-order perturbation of the density matrix $\gamma^{(1),\mathrm{LDA}}_{Z,N,W}$ in $\mathfrak{S}_{1,1}$.

3. Numerical method

In this section, we present the discretization method and the algorithms we used to calculate numerically the ground state density matrices for (9), (10), and (13) for cylindrically symmetric perturbation potentials W, together with the ground state energy and the lowest eigenvalues of the associated Kohn–Sham operator. From now on, we make the assumption that the ground state density of (13), if it exists,

[1] Note that $\epsilon^{0,\mathrm{rHF}}_{Z,N,\mathrm{F}} < 0$ whenever $0 < N < Z$ (see, e.g., [35]).

is cylindrically symmetric, which is always the case for the rHF model. Using spherical coordinates, we can write

$$W(r,\theta)=\sum_{l=0}^{+\infty} W_l(r)Y_l^0(\theta)\in\mathscr{H}^0$$

(since Y_l^0 is independent of φ, we use the notation $Y_l^0(\theta)$ instead of $Y_l^0(\theta,\varphi)$). As the ground state density $\rho_{Z,N,\beta W}$ is assumed to be cylindrically symmetric as well, one has

$$\rho_{Z,N,\beta W}(r,\theta)=\sum_{l=0}^{+\infty}\rho_{Z,N,\beta W,l}(r)Y_l^0(\theta).$$

The Hartree and the exchange-correlation potentials also have the same symmetry. For $\rho\in L^1(\mathbb{R}^3)\cap L^3(\mathbb{R}^3)\cap\mathscr{H}^0$, we have

$$V^{\mathrm{H}}(\rho)(r,\theta)=\sum_{l=0}^{+\infty}V^{\mathrm{H}}_{\rho_l}(r)Y_l^0(\theta)\quad\text{and}\quad v_{\mathrm{xc}}(\rho)(r,\theta)=\sum_{l=0}^{+\infty}(v_\rho^{\mathrm{xc}})_l(r)Y_l^0(\theta),$$

where, for each $l\geq 0$, $V^{\mathrm{H}}_{\rho_l}(r)$ solves the differential equation

$$-\frac{1}{r}\frac{d^2}{dr^2}(rV^{\mathrm{H}}_{\rho_l})+\frac{l(l+1)}{r^2}V^{\mathrm{H}}_{\rho_l}=4\pi\rho_l$$

with boundary conditions

$$\lim_{r\to 0^+} rV^{\mathrm{H}}_{\rho_l}(r)=0\quad\text{and}\quad\lim_{r\to+\infty} rV^{\mathrm{H}}_{\rho_l}(r)=\left(4\pi\int_0^{+\infty}r^2\rho_0(r)\,dr\right)\delta_{l0},$$

while $(v_\rho^{\mathrm{xc}})_l$ can be computed by projection on the spherical harmonics Y_l^0:

$$(v_\rho^{\mathrm{xc}})_l(r)=2\pi\int_0^{\pi}v_{\mathrm{xc}}(\rho)(r,\theta)Y_l^0(\theta)\sin\theta\,d\theta.$$

3.1. ***Discretization of the Kohn–Sham model.*** Recall that for $W\in\mathscr{W}_s$ and $\beta\neq 0$, the energy functional defined by (12) is not necessarily bounded below on $\mathscr{K}_N$, which implies in particular that (13) may have no ground state. Nevertheless, one can compute approximations of (13) in finite-dimensional spaces, provided that the basis functions decay fast enough at infinity. Let $N_h\in\mathbb{N}^*$ and $m_h\geq m_Z^*:=\max\{m\mid\text{there exists } k>0,\ \epsilon^0_{m,k}\leq\epsilon^0_{Z,N,\mathrm{F}}\}$, and let $\{\mathscr{X}_i\}_{1\leq i\leq N_h}\in(H_0^1(0,+\infty))^{N_h}$ be a free family of real-valued basis functions. We then introduce the finite-dimensional spaces

$$\mathscr{V}^{m,h}:=\mathscr{V}^m\cap\operatorname{span}_{\mathbb{R}}\left(\frac{\mathscr{X}_i(r)}{r}Y_l^m(\theta,\phi)\right)_{\substack{1\leq i\leq N_h\\ |m|\leq l\leq m_h}}\subset H^1(\mathbb{R}^3,\mathbb{C})\tag{18}$$

and

$$\mathscr{X}^h = \mathrm{span}_{\mathbb{R}}(\mathscr{X}_1, \dots, \mathscr{X}_{N_h}) \subset H_0^1(0, +\infty), \tag{19}$$

and the set

$$\mathscr{K}_{N,h} := \left\{ \gamma \in \mathscr{K}_N \;\middle|\; \gamma = \sum_{m=-m_h}^{m_h} \gamma^m,\ \gamma^m \in \mathscr{S}(\mathscr{H}^m),\ \mathrm{Ran}(\gamma^m) \subset \mathscr{V}^{m,h} \right\} \subset \mathscr{K}_N.$$

Note that since our goal is to compute nonmagnetic ground states, we are allowed to limit ourselves to real linear combinations in (18) and (19).

3.1.1. *Variational approximation.* A variational approximation of (13) is obtained by minimizing the energy functional (12) over the approximation set $\mathscr{K}_{N,h}$:

$$\widetilde{\mathscr{F}}^{\mathrm{rHF/LDA}}_{Z,N,h}(\beta W) := \inf\{\widetilde{E}^{\mathrm{rHF/LDA}}_{Z,N}(\gamma_h, \beta W) \mid \gamma_h \in \mathscr{K}_{N,h}\}. \tag{20}$$

Any $\gamma_h \in \mathscr{K}_{N,h}$ can be written as

$$\gamma_h = \sum_{\substack{-m_h \le m \le m_h \\ 1 \le k \le (m_h - |m| + 1)N_h}} n_{m,k} |\Phi_{m,k,h}\rangle\langle\Phi_{m,k,h}|, \tag{21}$$

with

$$\Phi_{m,k,h} \in \mathscr{V}^{m,h}, \qquad \int_{\mathbb{R}^3} \Phi_{m,k,h}\Phi^*_{m,k',h} = \delta_{kk'}, \qquad \Phi_{-m,k,h} = (-1)^m \Phi^*_{m,k,h},$$
$$0 \le n_{m,k} = n_{-m,k} \le 2, \qquad \sum_{\substack{-m_h \le m \le m_h \\ 1 \le k \le (m_h - |m| + 1)N_h}} n_{m,k} = N.$$

The functions $\Phi_{m,k,h}$, being in $\mathscr{V}^{m,h}$, are of the form

$$\Phi_{m,k,h}(r, \theta, \varphi) = \sum_{l=|m|}^{m_h} \frac{u_l^{m,k,h}(r)}{r} Y_l^m(\theta, \varphi), \tag{22}$$

where for each $-m_h \le m \le m_h$, $1 \le k \le (m_h - |m| + 1)N_h$ and $|m| \le l \le m_h$, $u_l^{m,k,h} \in \mathscr{X}^h$. Note that $u_l^{-m,k,h} = u_l^{m,k,h}$. Expanding the functions $u_l^{m,k,h}$ in the basis $(\mathscr{X}_i)_{1 \le i \le N_h}$ as

$$u_l^{m,k,h}(r) = \sum_{i=1}^{N_h} U_{i,l}^{m,k} \mathscr{X}_i(r), \tag{23}$$

and gathering the coefficients $U_{i,l}^{m,k}$ for fixed m and k in a rectangular matrix $U^{m,k} \in \mathbb{R}^{N_h \times (m_h - |m| + 1)}$, any $\gamma_h \in \mathscr{K}_{N,h}$ can be represented via (21)–(23) by at least one element of the set

$$\mathscr{M}_{N,h} := \mathscr{U}_h \times \mathscr{N}_{N,h}, \tag{24}$$

where

$$\mathcal{U}_h := \Big\{ (U^{m,k})_{\substack{-m_h \le m \le m_h \\ 1 \le k \le (m_h - |m| + 1) N_h}} \Big| \; U^{m,k} = U^{-m,k} \in \mathbb{R}^{N_h \times (m_h - |m| + 1)}, \; \mathrm{Tr}([U^{m,k}]^T M_0 U^{m,k'}) = \delta_{kk'} \Big\},$$

and

$$\mathcal{N}_{N,h} := \Big\{ (n_{m,k})_{\substack{-m_h \le m \le m_h \\ 1 \le k \le (m_h - |m| + 1) N_h}} \Big| \; 0 \le n_{m,k} = n_{-m,k} \le 2, \sum_{\substack{-m_h \le m \le m_h \\ 1 \le k \le (m_h - |m| + 1) N_h}} n_{m,k} = N \Big\}.$$

The matrix M_0 appearing in the definition of $\mathcal{U}_h$ is the mass matrix defined by

$$[M_0]_{ij} = \int_0^{+\infty} \mathcal{X}_i \mathcal{X}_j,$$

and the constraints $\mathrm{Tr}([U^{m,k}]^T M_0 U^{m,k'}) = \delta_{kk'}$ come from the fact that

$$\begin{aligned} \int_{\mathbb{R}^3} \Phi_{m,k,h} \Phi^*_{m,k',h} &= \int_0^{+\infty} \int_{\mathbb{S}^2} \Big(\sum_{l=|m|}^{m_h} \sum_{i=1}^{N_h} U^{m,k}_{i,l} \frac{\mathcal{X}_i(r)}{r} Y^m_l(\sigma) \Big) \\ &\qquad \times \Big(\sum_{l'=|m|}^{m_h} \sum_{i=1}^{N_h} U^{m,k'}_{j,l'} \frac{\mathcal{X}_j(r)}{r} Y^m_{l'}(\sigma)^* \Big) r^2 \, d\sigma \, dr \\ &= \sum_{l=|m|}^{m_h} \sum_{i,j=1}^{N_h} U^{m,k}_{i,l} [M_0]_{ij} U^{m,k'}_{j,l} = \mathrm{Tr}([U^{m,k}]^T M_0 U^{m,k'}). \end{aligned}$$

Remark. An interesting observation is that, if there is no accidental degeneracy in the set of the occupied energy levels of $H^{0,\mathrm{rHF/LDA}}_{Z,N}$, and if the occupied orbitals are well enough approximated in the space $\mathcal{V}^{m,h}$, then the approximate ground state density matrix $\gamma^{0,\mathrm{rHF/LDA}}_{Z,N,h}$ has a unique representation of the form (21)–(23), up to the signs and the numbering of the functions $u^{m,k,h}_l$, that is, up to the signs and numbering of the column vectors of the matrices $U^{m,k}$. By continuity, this uniqueness of the representation will survive if a small-enough cylindrically symmetric perturbation is turned on. This is the reason why this representation is well suited to our study.

Let us now express each component of the energy functional $\widetilde{E}^{\mathrm{rHF,LDA}}_{Z,N}(\gamma_h, \beta W)$ using the representation (21)–(23) of the elements of $\mathcal{K}_{N,h}$. For this purpose, we introduce the $N_h \times N_h$ real symmetric matrices A and M_n, $n = -2, -1, 0, 1$, with entries

$$A_{ij} = \int_0^{+\infty} \mathcal{X}'_i \mathcal{X}'_j \quad \text{and} \quad [M_n]_{ij} = \int_0^{+\infty} r^n \mathcal{X}_i(r) \mathcal{X}_j(r) \, dr. \tag{25}$$

The weighted mass matrices M_{-2} and M_{-1} are well defined in view of the Hardy inequality,

$$\text{for all } u \in H_0^1(0,+\infty), \qquad \int_0^{+\infty} \frac{u^2(r)}{r^2}\,dr \le 4\pi \int_0^{+\infty} |u'|^2.$$

We assume from now on that the basis functions $\mathscr{X}_i$ decay fast enough at infinity for the weighted mass matrix M_1 to be well defined.

In the representation (21)–(23), the kinetic energy is equal to

$$\tfrac{1}{2}\operatorname{Tr}(-\Delta\gamma_h) = \frac{1}{2} \sum_{\substack{-m_h \le m \le m_h \\ 1 \le k \le (m_h - |m| + 1)\times N_h}} n_{m,k}\big(\operatorname{Tr}([U^{m,k}]^T A U^{m,k}) + \operatorname{Tr}(D_m [U^{m,k}]^T M_{-2} U^{m,k})\big), \tag{26}$$

where $D_m \in \mathbb{R}^{(m_h - |m| + 1)\times(m_h - |m| + 1)}$ is the diagonal matrix defined by

$$D_m = \operatorname{diag}(|m|(|m|+1), \dots, m_h(m_h+1)). \tag{27}$$

All the other terms in the energy functional depending on the density

$$\rho_h := \rho_{\gamma_h} = \sum_{\substack{-m_h \le m \le m_h \\ 1 \le k \le (m_h - |m| + 1) N_h}} n_{m,k} |\Phi_{m,k,h}|^2, \tag{28}$$

we first need to express this quantity as a function of the matrices $U^{m,k}$ and the occupation numbers $n_{m,k}$. As the function ρ_h is in $\mathscr{H}^0$, we have

$$\rho_h(r,\theta) = \sum_{l=0}^{2m_h} \rho_l^h(r) Y_l^0(\theta). \tag{29}$$

Inserting (22) in (28), we get

$$\rho_h(r,\theta) = \sum_{\substack{-m_h \le m \le m_h \\ 1 \le k \le (m_h - |m| + 1) N_h}} n_{m,k} \left| \sum_{l=|m|}^{m_h} \frac{u_l^{m,k,h}(r)}{r} Y_l^m(\theta,\varphi) \right|^2. \tag{30}$$

We recall the equality [32]

$$Y_{l_1}^m (Y_{l_2}^m)^* = (-1)^m Y_{l_1}^m Y_{l_2}^{-m} = \sum_{l_3 = |l_1 - l_2|}^{l_1 + l_2} c_{l_1,l_2,l_3}^m Y_{l_3}^0, \tag{31}$$

with

$$c_{l_1,l_2,l_3}^m = (-1)^m \sqrt{\frac{(2l_1+1)(2l_2+1)(2l_3+1)}{4\pi}} \begin{pmatrix} l_1 & l_2 & l_3 \\ m & -m & 0 \end{pmatrix} \begin{pmatrix} l_1 & l_2 & l_3 \\ 0 & 0 & 0 \end{pmatrix},$$

where $\left(\begin{smallmatrix} l_1 & l_2 & l_3 \\ m_1 & m_2 & m_3 \end{smallmatrix}\right)$ denote the Wigner 3j-symbols. Inserting the expansion (23) in (30) and using (31) and the fact that

$$\begin{pmatrix} l_1 & l_2 & l_3 \\ m_1 & m_2 & m_3 \end{pmatrix} = 0 \quad \text{unless } |l_1 - l_2| \le l_3 \le l_1 + l_2,$$

we obtain

$$\rho_h(r,\theta) = \sum_{l=0}^{2m_h} \Bigg[\sum_{i,j=1}^{N_h} \Bigg(\sum_{\substack{-m_h \le m \le m_h \\ 1 \le k \le (m_h - |m| + 1) \times N_h}} n_{m,k} \sum_{l',l''=|m|}^{m_h} c^m_{l',l'',l} U^{m,k}_{i,l'} U^{m,k}_{j,l''} \Bigg) \times \frac{\mathscr{X}_i(r)}{r} \frac{\mathscr{X}_j(r)}{r} \Bigg] Y^0_l(\theta),$$

from which we conclude that

$$\rho^h_l(r) = \sum_{i,j=1}^{N_h} \Bigg(\sum_{\substack{-m_h \le m \le m_h \\ 1 \le k \le (m_h - |m| + 1) \times N_h}} n_{m,k} \sum_{l',l''=|m|}^{m_h} c^m_{l',l'',l} U^{m,k}_{i,l'} U^{m,k}_{j,l''} \Bigg) \frac{\mathscr{X}_i(r)}{r} \frac{\mathscr{X}_j(r)}{r}.$$

For $0 \le l \le 2m_h$, we introduce the matrix $R_l \in \mathbb{R}^{N_h \times N_h}$ defined by

$$R_l := \sum_{\substack{-m_h \le m \le m_h \\ 1 \le k \le (m_h - |m| + 1) \times N_h}} n_{m,k} U^{m,k} C^{l,m} [U^{m,k}]^T \tag{32}$$

where $C^{l,m} \in \mathbb{R}^{(m_h - |m| + 1) \times (m_h - |m| + 1)}$ is the symmetric matrix[2] defined by,

$$\text{for all } |m| \le l \le 2m_h, \quad C^{l,m}_{l',l''} = \sqrt{4\pi}\, c^m_{l',l'',l}, \tag{33}$$

so that

$$\rho_h(r,\theta) = \frac{1}{\sqrt{4\pi}} \sum_{l=0}^{2m_h} \sum_{i,j=1}^{N_h} [R_l]_{i,j} \frac{\mathscr{X}_i(r)}{r} \frac{\mathscr{X}_j(r)}{r} Y^0_l(\theta). \tag{34}$$

Note that $C^{0,m}$ is the identity matrix, so that

$$R_0 = \sum_{\substack{-m_h \le m \le m_h \\ 1 \le k \le (m_h - |m| + 1) \times N_h}} n_{m,k} U^{m,k} [U^{m,k}]^T$$

and

$$\operatorname{Tr}(M_0 R_0) = \sum_{\substack{-m_h \le m \le m_h \\ 1 \le k \le (m_h - |m| + 1) \times N_h}} n_{m,k} \operatorname{Tr}(M_0 U^{m,k} [U^{m,k}]^T) = \sum_{\substack{-m_h \le m \le m_h \\ 1 \le k \le (m_h - |m| + 1) \times N_h}} n_{m,k} = N,$$

[2]The symmetry of the matrix C^{lm} comes from the symmetry properties of the 3j-symbols

$$\begin{pmatrix} l_1 & l_2 & l_3 \\ m_1 & m_2 & m_3 \end{pmatrix} = (-1)^{l_1+l_2+l_3} \begin{pmatrix} l_2 & l_1 & l_3 \\ m_2 & m_1 & m_3 \end{pmatrix} = (-1)^{l_1+l_2+l_3} \begin{pmatrix} l_2 & l_1 & l_3 \\ -m_2 & -m_1 & -m_3 \end{pmatrix}.$$

and that $C^{1,m}$ is a symmetric tridiagonal matrix whose diagonal elements all are equal to zero.

The Coulomb attraction energy between the nucleus and the electrons then is equal to

$$\begin{aligned}
-Z\int_{\mathbb{R}^3}\frac{\rho_h}{|\cdot|} &= -Z\int_0^{+\infty}\int_{\mathbb{S}^2}\frac{1}{r}\left(\frac{1}{\sqrt{4\pi}}\sum_{l=0}^{2m_h}\sum_{i,j=1}^{N_h}[R_l]_{i,j}\frac{\mathscr{X}_i(r)}{r}\frac{\mathscr{X}_j(r)}{r}Y_l^0(\sigma)\right)r^2\,dr\,d\sigma\\
&= -Z\int_0^{+\infty}\int_{\mathbb{S}^2}\frac{1}{r}\left(\sum_{l=0}^{2m_h}\sum_{i,j=1}^{N_h}[R_l]_{i,j}\frac{\mathscr{X}_i(r)}{r}\frac{\mathscr{X}_j(r)}{r}Y_l^0(\sigma)\right)Y_0^0(\sigma)^*r^2\,dr\,d\sigma\\
&= -Z\sum_{i,j=1}^{N_h}[R_0]_{i,j}[M_{-1}]_{ij} = -Z\,\mathrm{Tr}(M_{-1}R_0),
\end{aligned}$$

where we have used the orthonormality condition (15) and the fact that $Y_0^0 = 1/\sqrt{4\pi}$.

Likewise, since $Y_1^0(\theta) = \sqrt{3/(4\pi)}\cos(\theta)$, the Stark potential (17) can be written in spherical coordinates as

$$W_{\mathrm{Stark}}(r,\theta) = -\sqrt{\frac{4\pi}{3}}rY_1^0(\theta) = -\sqrt{\frac{4\pi}{3}}rY_1^0(\theta)^*,$$

and the potential energy due to the external electric field is then equal to

$$\beta\int_{\mathbb{R}^3}\rho_h W_{\mathrm{Stark}} = -\frac{1}{\sqrt{3}}\beta\sum_{i,j=1}^{N_h}[R_1]_{ij}[M_1]_{ij} = -\frac{1}{\sqrt{3}}\beta\,\mathrm{Tr}(M_1R_1).$$

Let μ be a radial, continuous function from $\mathbb{R}^3$ to $\mathbb{R}$ vanishing at infinity and such that $\int_{\mathbb{R}^3}\mu = 1$. The Coulomb interaction energy can be rewritten as

$$\tfrac{1}{2}D(\rho_h,\rho_h) = \tfrac{1}{2}D\left(\rho_h - \left(\int_{\mathbb{R}^3}\rho_h\right)\mu,\ \rho_h - \left(\int_{\mathbb{R}^3}\rho_h\right)\mu\right) + ND(\mu,\rho_h) - \frac{N^2}{2}D(\mu,\mu). \tag{35}$$

The reason why we introduce the charge distribution μ is to make neutral the charge distributions $\rho_h - \left(\int_{\mathbb{R}^3}\rho_h\right)\mu$ in the first term of the right-hand side of (35), in such a way that the physical solution Q_{0,R_0} to (38) below for $l=0$ is in $H_0^1(0,+\infty)$.

Introducing the real symmetric matrix $V_\mu \in \mathbb{R}^{N_h\times N_h}$ with entries

$$[V_\mu]_{ij} = \int_0^{+\infty}[V^{\mathrm{H}}(\mu)](r\boldsymbol{e})\mathscr{X}_i(r)\mathscr{X}_j(r)\,dr, \tag{36}$$

where $\boldsymbol{e}$ is any unit vector of $\mathbb{R}^3$ (the value of $V^{\mathrm{H}}(\mu)(r\boldsymbol{e})$ is independent of $\boldsymbol{e}$ since $V^{\mathrm{H}}(\mu)$ is radial), the sum of the last two terms of the right-hand side of (35) can

be rewritten as

$$N D(\mu, \rho_h) - \frac{N^2}{2} D(\mu, \mu) = N \operatorname{Tr}(V_\mu R_0) - \frac{N^2}{2} D(\mu, \mu).$$

Denoting by

$$\widetilde{V}^{\mathrm{H}}(\rho_h) = V^{\mathrm{H}}(\rho_h - \left(\int_{\mathbb{R}^3} \rho_h\right)\mu),$$

we have by symmetry $\widetilde{V}^{\mathrm{H}}(\rho_h) \in \mathscr{H}^0$ and

$$[\widetilde{V}^{\mathrm{H}}(\rho_h)](r, \theta) = \sum_{l=0}^{2m_h} \widetilde{V}_l(\rho_l^h)(r) Y_l^0(\theta) = \sum_{l=0}^{2m_h} \frac{Q_{l,R_l}(r)}{r} Y_l^0(\theta),$$

where Q_{l,R_l} is the unique solution in $H_0^1(0, +\infty)$ to the differential equation

$$-\frac{d^2 Q_{l,R_l}}{dr^2}(r) + \frac{l(l+1)}{r^2} Q_{l,R_l}(r) = 4\pi r \left(\left(\frac{1}{\sqrt{4\pi}} \sum_{i,j=1}^{N_h} [R_l]_{ij} \frac{\mathscr{X}_i(r)\mathscr{X}_j(r)}{r^2}\right) - N\mu(r)\delta_{l0}\right). \quad (37)$$

Note that the mappings $R_l \mapsto Q_{l,R_l}$ are linear. We therefore obtain

$$\tfrac{1}{2} D(\rho_h, \rho_h) = \frac{1}{2} \sum_{l=0}^{2m_h} \frac{1}{4\pi} \left(\int_0^{+\infty} \left(\left(\frac{dQ_{l,R_l}}{dr}(r)\right)^2 + \frac{l(l+1)}{r^2} Q_{l,R_l}(r)^2\right) dr\right) + N \operatorname{Tr}(V_\mu R_0) - \frac{N^2}{2} D(\mu, \mu). \quad (38)$$

Finally, the exchange-correlation energy is

$$E_{\mathrm{xc}}(\rho_h) = 2\pi \int_0^{+\infty} \int_0^{\pi} \epsilon_{\mathrm{xc}}\left(\frac{1}{\sqrt{4\pi}} \sum_{l=0}^{2m_h} \sum_{i,j=1}^{N_h} [R_l]_{ij} \frac{\mathscr{X}_i(r)}{r} \frac{\mathscr{X}_j(r)}{r} Y_l^0(\theta)\right) r^2 \sin\theta \, dr \, d\theta. \quad (39)$$

3.1.2. *Approximation of the Hartree term.* Except for very specific basis functions (such as Gaussian atomic orbitals), it is not possible to evaluate exactly the first contribution to the Coulomb energy (38). It is therefore necessary to approximate it. For this purpose, we use a variational approximation of (37)–(38) in an auxiliary basis set $\{\zeta_p\}_{1 \le p \le N_{h,\mathrm{a}}} \in (H_0^1(0, +\infty))^{N_{h,\mathrm{a}}}$, which amounts to replacing $\frac{1}{2} D(\rho_h, \rho_h)$ by its lower bound

$$\frac{1}{2} D_h(\rho_h, \rho_h) = \frac{1}{8\pi} \left(\int_0^{+\infty} \left(\left(\frac{dQ_{l,R_l}^h}{dr}(r)\right)^2 + \frac{l(l+1)}{r^2} Q_{l,R_l}^h(r)^2\right) dr\right) + N \operatorname{Tr}(V_\mu R_0) - \frac{N^2}{2} D(\mu, \mu), \quad (40)$$

where Q^h_{l,R_l} is the unique solution in $\zeta^h = \mathrm{span}(\zeta_1, \dots, \zeta_{N_{h,\mathrm{a}}})$ to the problem,

$$\text{for all } v_h \in \zeta^h, \quad \int_0^{+\infty} \left(\frac{dQ^h_{l,R_l}}{dr}(r) \frac{dv_h}{dr}(r) + \frac{l(l+1)}{r^2} Q^h_{l,R_l}(r) v_h(r) \right) dr$$
$$= 4\pi \int_0^{+\infty} r \left(\left(\frac{1}{\sqrt{4\pi}} \sum_{i,j=1}^{N_h} [R_l]_{ij} \frac{\mathscr{X}_i(r)\mathscr{X}_j(r)}{r^2} \right) - N\mu(r)\delta_{l0} \right) v_h(r) dr,$$

which is nothing but the variational approximation of (37) in the finite-dimensional space ζ^h. Expanding the functions Q^h_{l,R_l} in the basis set $\{\zeta_k\}_{1 \le k \le N_{h,\mathrm{a}}}$ as

$$Q^h_{l,R_l}(r) = \sum_{p=1}^{N_{h,\mathrm{a}}} Q_{p,l} \zeta_p(r),$$

and collecting the coefficients $Q_{p,l}$, $1 \le k \le N_{h,\mathrm{a}}$, in a vector $Q_l \in \mathbb{R}^{N_{h,\mathrm{a}}}$, we obtain that the vector Q_l is the solution to the linear system

$$(A^{\mathrm{a}} + l(l+1) M^{\mathrm{a}}_{-2}) Q_l = 4\pi (F : R_l - N\delta_{l0} G), \tag{41}$$

where the $N_{h,\mathrm{a}} \times N_{h,\mathrm{a}}$ real symmetric matrices A^{a} and M^{a}_{-2} are defined by

$$A^{\mathrm{a}}_{pq} = \int_0^{+\infty} \zeta_p' \zeta_q', \qquad [M^{\mathrm{a}}_{-2}]_{pq} = \int_0^{+\infty} \frac{\zeta_p(r)\zeta_q(r)}{r^2} dr, \tag{42}$$

where $F \in \mathbb{R}^{N_{h,\mathrm{a}} \times N_h \times N_h}$ is the three-index tensor with entries

$$F_{pij} = \frac{1}{\sqrt{4\pi}} \int_0^{+\infty} \frac{\mathscr{X}_i(r)\mathscr{X}_j(r)\zeta_p(r)}{r} dr, \tag{43}$$

and where $G \in \mathbb{R}^{N_{h,\mathrm{a}}}$ is the vector with entries

$$G_p = \int_0^{+\infty} r\mu(r)\zeta_p(r)\, dr. \tag{44}$$

Note that since $N = \mathrm{Tr}(M_0 R_0)$, the mappings $R_l \mapsto Q_l$ are in fact linear. We finally get

$$\tfrac{1}{2} D_h(\rho_h, \rho_h) = \frac{1}{8\pi} \sum_{l=0}^{2m_h} Q_l^T (A^{\mathrm{a}} + l(l+1) M^{\mathrm{a}}_{-2}) Q_l + N\, \mathrm{Tr}(V_\mu R_0) - \frac{N^2}{2} D(\mu, \mu), \tag{45}$$

where Q_l is the solution to (41).

3.1.3. *Final form of the discretized problem and Euler–Lagrange equations.* We therefore end up with the following approximation of problem (13):

$$\widetilde{\mathscr{F}}^{\mathrm{rHF/LDA}}_{Z,N,h}(\beta W) := \inf\Big\{ \mathscr{E}^{\mathrm{rHF/LDA}}_{Z,N,\beta}((U^{m,k}), (n_{m,k})) \;\Big|\; (U^{m,k})_{\substack{-m_h \le m \le m_h \\ 1 \le k \le (m_h - |m| + 1)N_h}} \in \mathscr{U}_h, \; (n_{m,k})_{\substack{-m_h \le m \le m_h \\ 1 \le k \le (m_h - |m| + 1)N_h}} \in \mathscr{N}_{N,h} \Big\}, \tag{46}$$

where

$$
\begin{aligned}
&\mathscr{E}^{\mathrm{rHF/LDA}}_{Z,N,\beta}((U^{m,k}),(n_{m,k})) \\
&\quad := \frac{1}{2} \sum_{\substack{-m_h \le m \le m_h \\ 1 \le k \le (m_h - |m| + 1)N_h}} n_{m,k}(\mathrm{Tr}([U^{m,k}]^T A U^{m,k}) + \mathrm{Tr}(D_m [U^{m,k}]^T M_{-2} U^{m,k})) \\
&\qquad - Z\,\mathrm{Tr}(M_{-1} R_0) + \frac{1}{8\pi} \sum_{l=0}^{2m_h} Q_l^T (A^{\mathrm{a}} + l(l+1) M^{\mathrm{a}}_{-2}) Q_l + N\,\mathrm{Tr}(V_\mu R_0) \\
&\qquad - \frac{N^2}{2} D(\mu,\mu) + E_{\mathrm{xc}}(\rho_h) - \frac{\beta}{\sqrt{3}} \mathrm{Tr}(M_1 R_1),
\end{aligned}
$$

where for each l, the matrix R_l and the vector Q_l are defined by (32) and (41), respectively, and where the second-to-last term in the right-hand side is given by (39).

The gradient of $\mathscr{E}^{\mathrm{rHF/LDA}}_{Z,N,\beta}$ with respect to $U^{m,k}$ is

$$
\begin{aligned}
\nabla_{U^{m,k}} \mathscr{E}^{\mathrm{rHF/LDA}}_{Z,N,\beta} = 2n_{m,k} \Bigg(& \tfrac{1}{2} A U^{m,k} + \tfrac{1}{2} M_{-2} U^{m,k} D_m - Z M_{-1} U^{m,k} + N V_\mu U^{m,k} \\
& + \sum_{l=0}^{2m_h} (Q_l^T \cdot F)(U^{m,k} C^{l,m}) + \sum_{l=0}^{2m_h} V^l_{\mathrm{xc}} U^{m,k} C^{l,m} \\
& - \frac{\beta}{\sqrt{3}} M_1 U^{m,k} C^{1,m} \Bigg),
\end{aligned}
$$

where for each $0 \le l \le 2m_h$, the $N_h \times N_h$ real matrix V^l_{xc} is defined by

$$
\begin{aligned}
[V^l_{\mathrm{xc}}]_{ij} = \sqrt{\pi} \int_0^{+\infty} \int_0^{\pi} v_{\mathrm{xc}} \Bigg(\frac{1}{\sqrt{4\pi}} \sum_{i,j=1}^{N_h} [R_l]_{ij} \frac{\mathscr{X}_i(r)\mathscr{X}_j(r)}{r^2} \Bigg) \\
\times \mathscr{X}_i(r)\mathscr{X}_j(r) Y_l^0(\theta)\, \sin\theta\, dr\, d\theta, \qquad (47)
\end{aligned}
$$

where $v_{\mathrm{xc}}(\rho) := \frac{d\epsilon_{\mathrm{xc}}}{d\rho}(\rho)$ is the exchange-correlation potential.

Diagonalizing simultaneously the Kohn–Sham Hamiltonian and the ground state density matrix in an orthonormal basis, we obtain that the ground state can be obtained by solving the following system of first-order optimality conditions, which is nothing but a reformulation of the discretized extended Kohn–Sham equations

exploiting the cylindrical symmetry of the problem:

$$\tfrac{1}{2}AU^{m,k} + \tfrac{1}{2}M_{-2}U^{m,k}D_m - ZM_{-1}U^{m,k} + NV_\mu U^{m,k} + \sum_{l=0}^{2m_h}(Q_l^T \cdot F)(U^{m,k}C^{l,m}) + \sum_{l=0}^{2m_h} V_{\mathrm{xc}}^l U^{m,k}C^{l,m} - \frac{1}{\sqrt{3}}\beta M_1 U^{m,k}C^{1,m} = \epsilon_{m,k}M_0U^{m,k}, \tag{48}$$

$$\mathrm{Tr}([U^{m,k}]^T M_0 U^{m,k'}) = \delta_{kk'}, \tag{49}$$

$$(A^{\mathrm{a}} + l(l+1)M_{-2}^{\mathrm{a}})Q_l = F : R_l - \mathrm{Tr}(M_0R_0)\delta_{l0}G, \tag{50}$$

$$[V_{\mathrm{xc}}^l]_{ij} = \sqrt{\pi}\int_0^{+\infty}\int_0^{\pi} v_{\mathrm{xc}}\left(\frac{1}{\sqrt{4\pi}}\sum_{i,j=1}^{N_h}[R_l]_{ij}\frac{\mathscr{X}_i(r)\mathscr{X}_j(r)}{r^2}\right) \times \mathscr{X}_i(r)\mathscr{X}_j(r)Y_l^0(\theta)\sin\theta\, dr\, d\theta, \tag{51}$$

$$n_{m,k} = 2 \text{ if } \epsilon_{m,k} < \epsilon_{\mathrm{F}}, \quad 0 \le n_{m,k} \le 2 \text{ if } \epsilon_{m,k} = \epsilon_{\mathrm{F}}, \quad n_{m,k} = 0 \text{ if } \epsilon_{m,k} > \epsilon_{\mathrm{F}}, \tag{52}$$

$$\sum_{\substack{-m_h \le m \le m_h \\ 1 \le k \le (m_h - |m| + 1)N_h}} n_{m,k} = N, \tag{53}$$

$$R_l = \sum_{\substack{-m_h \le m \le m_h \\ 1 \le k \le (m_h - |m| + 1)N_h}} n_{m,k}U^{m,k}C^{l,m}[U^{m,k}]^T, \tag{54}$$

where the matrices A, M_{-2}, M_{-1}, M_0, M_1, D_m, V_μ, A^{a}, M_{-2}^{a}, and $C^{l,m}$, the 3-index tensor F, and the vector G are defined by (25), (27), (33), (36), (42), (43), and (44).

3.1.4. $\mathbb{P}_4$ *finite element method.* In our calculations, we use the same approximation space to discretize the radial components of the Kohn–Sham orbitals and the radial Poisson equations (37), so that, in our implementation of the method, $N_{h,\mathrm{a}} = N_h$ and $\mathscr{X}^h = \zeta^h$. We choose a cut-off radius $L_e > 0$ large enough and discretize the interval $[0, L_e]$ using a nonuniform grid with $N_I + 1$ points $0 = r_1 < r_2 < \cdots < r_{N_I} < r_{N_I+1} = L_e$. The positions of the points are chosen according to the rule

$$r_k = r_{k-1} + h_k, \qquad h_{N_I} = \frac{1-s}{1-s^{N_I}}L_e, \qquad h_{k-1} = sh_k,$$

where $0 < s < 1$ is a scaling parameter leading to a progressive refinement of the mesh when one gets closer to the nucleus ($r = 0$). To achieve the desired accuracy, we use the $\mathbb{P}_4$ finite element method.

All the terms in the variational discretization of the energy and of the constraints can be computed exactly (up to finite arithmetic errors), except the exchange-correlation terms (39) and (47), which require a numerical quadrature method. In

our calculation, we use Gaussian quadrature formulas [37] of the form

$$\int_0^{+\infty}\int_0^{\pi} f(r,\theta)\sin\theta\, dr\, d\theta = \int_0^{+\infty}\int_{-1}^{1} f(r,\arccos t_\theta)\, dr\, dt_\theta$$
$$\simeq \sum_{k=1}^{N_I}\sum_{i=1}^{N_{\mathrm{g},r}}\sum_{j=1}^{N_{\mathrm{g},\theta}} h_k w_{i,\mathrm{r}} w_{j,\theta} f(r_k + h_k t_{i,\mathrm{r}}, \arccos(t_{j,\theta})),$$

where the $0 < t_{1,r} < \cdots < t_{N_{\mathrm{g},r},r} < 1$ and $-1 < t_{1,\theta} < \cdots < t_{N_{\mathrm{g},\theta},\theta} < 1$ are Gauss points for the r-variable and t_θ-variable with associated weights $w_{1,r}, \ldots, w_{N_{\mathrm{g},r},r}$ and $w_{1,\theta}, \ldots, w_{N_{\mathrm{g},\theta},\theta}$, respectively.

More details about the practical implementation of the method are provided in [9].

3.2. ***Description of the algorithm.*** In order to solve the self-consistent equations (48)–(54), we use an iterative algorithm. For clarity, we first present this algorithm within the continuous setting. Its formulation in the discretized setting considered here is detailed below. The iterations are defined as follows with an Ansatz of the ground state density $\rho^{[n]}$ being known.

(1) Construct the Kohn–Sham operator

$$H^{[n]} = -\tfrac{1}{2}\Delta - \frac{Z}{|\cdot|} + V^{\mathrm{H}}(\rho^{[n]}) + v_{\mathrm{xc}}(\rho^{[n]}) + \beta W$$

where $v_{\mathrm{xc}} = 0$ for the rHF model and $v_{\mathrm{xc}} = v_{\mathrm{xc}}^{\mathrm{LDA}}$ for the Kohn–Sham LDA model.

(2) For each $m \in \mathbb{Z}$, compute the negative eigenvalues of $H_m^{[n]} := \Pi_m H^{[n]} \Pi_m$, where Π_m is the orthogonal projector on the space $\mathscr{H}^m$:

$$H_m^{[n]}\phi_{m,k}^{[n+1]} = \epsilon_{m,k}^{[n+1]}\phi_{m,k}^{[n+1]}, \qquad \int_{\mathbb{R}^3} \phi_{m,k}^{[n+1]*}\phi_{m,k'}^{[n+1]} = \delta_{kk'}.$$

(3) Construct a new density

$$\rho_*^{[n+1]} = \sum_{m,k} n_{m,k}^{[n+1]} |\phi_{m,k}^{[n+1]}|^2,$$

where

$$\begin{cases} n_{m,k}^{[n+1]} = 2 & \text{if } \epsilon_{m,k}^{[n+1]} < \epsilon_{\mathrm{F}}^{[n+1]}, \\ 0 \le n_{m,k}^{[n+1]} \le 2 & \text{if } \epsilon_{m,k}^{[n+1]} = \epsilon_{\mathrm{F}}^{[n+1]}, \\ n_{m,k}^{[n+1]} = 0 & \text{if } \epsilon_{m,k}^{[n+1]} > \epsilon_{\mathrm{F}}^{[n+1]}, \end{cases} \quad \text{and} \quad \sum_{(m,k)} n_{m,k}^{[n+1]} = N.$$

(4) Update the density:

$$\rho^{[n+1]} = t_n \rho_*^{[n+1]} + (1 - t_n)\rho^{[n]},$$

where $t_n \in [0, 1]$ either is a fixed parameter independent of n and chosen a priori, or is optimized using the optimal damping algorithm (see below).

(5) If some convergence criterion is satisfied, then stop; else, replace n with $n+1$ and go to step (1).

In the nondegenerate case, that is, when $\epsilon_{\mathrm{F}}^{[n+1]}$ is not an eigenvalue of the Hamiltonian $H^{[n]}$, the occupation numbers $n_{m,k}^{[n+1]}$ are equal to either 0 (unoccupied) or 2 (fully occupied), while in the degenerate case the occupation numbers at the Fermi level have to be determined. We distinguish two cases: if $W = 0$, or more generally if W is spherically symmetric, and if $\epsilon_{\mathrm{F}}^{[n+1]}$ is not an accidentally degenerate eigenvalue of $H^{[n]}$, then the occupation numbers at the Fermi level are all equal; otherwise, the occupation numbers are not known a priori. In our approach we select the occupation numbers at the Fermi level which provide the lowest Kohn–Sham energy. When the degenerate eigenspace at the Fermi level is of dimension 3, that is, when the highest-energy partially occupied orbitals are perturbations of a three-fold degenerate p-orbital, the optimal occupation numbers can be found by using the golden search or bisection method [30, Chapter 10] since, in this case, the search space can be parametrized by a single real-valued parameter (this is due to the fact that the sum of the three occupation numbers is fixed and that two of them are equal by cylindrical symmetry). In the general case, more generic optimization methods have to be resorted to.

In the discretization framework we have chosen, the algorithm can be formulated as follows.

Initialization.

(1) Choose the numerical parameters m_h (cut-off in the spherical harmonics expansion), L_e (size of the simulation domain for the radial components of the Kohn–Sham orbitals and the electrostatic potential), N_I (size of the mesh for solving the radial equations), $N_{\mathrm{g},r}$ (number of Gauss points for the radial quadrature formula), $N_{\mathrm{g},\theta}$ (number of Gauss points for the angular quadrature formula), and $\varepsilon > 0$ (convergence threshold).

(2) Assemble the matrices $A = A^{\mathrm{a}}$, $M_{-2} = M_{-2}^{\mathrm{a}}$, M_{-1}, M_0, M_1, $C^{l,m}$, and V_μ and the vector G. The tensor F can be either computed once and for all, or the contractions $F : R_l^{[n]}$ can be computed on the fly, depending on the size of the discretization parameters and the computational means available.

(3) Choose an initial guess $(R_l^{[0]})_{0 \le l \le 2m_h}$ for the matrices representing the discretized ground state density at iteration 0 (it is possible to take $R_l = 0$ for all l if no other better guess is known).

Iterations. Assume the matrices $(R_l^{[n]})_{0\le l\le 2m_h}$ at iteration n are known.

(1) Construct the building blocks of the discretized analogues of the operators $H_m^{[n]}$. For this purpose,

(a) solve, for each $l = 0, \dots, 2m_h$, the linear equation

$$(A^{\mathrm{a}} + l(l+1)M_{-2}^{\mathrm{a}})Q_l^{[n]} = 4\pi(F : R_l^{[n]} - N\delta_{l0}G)$$

and

(b) assemble, for each $l = 0, \dots, 2m_h$, the matrix $V_l^{\mathrm{xc},[n]}$ by Gauss quadrature rules

$$[V_{\mathrm{xc}}^{l,[n]}]_{ij} = \sqrt{\pi}\sum_{k=1}^{N_I}\sum_{p=1}^{N_{\mathrm{g},r}}\sum_{q=1}^{N_{\mathrm{g},\theta}} h_k w_{p,\mathrm{r}} w_{q,\theta} f_{ij}^l(r_k + h_k t_{p,\mathrm{r}}, t_{q,\theta}),$$

where

$$f_{ij}^l(r, t_\theta) = v_{\mathrm{xc}}\left(\frac{1}{\sqrt{4\pi}}\sum_{l=0}^{m_h}\sum_{i,j=1}^{N_h}[R_l]_{i,j}\frac{\mathscr{X}_i(r)\mathscr{X}_j(r)}{r^2}Y_l^0(\arccos t_\theta)\right) \times \mathscr{X}_i(r)\mathscr{X}_j(r)Y_l^0(\arccos t_\theta).$$

(2) Solve, for each $0 \le m \le m_h$, the generalized eigenvalue problem

$$\begin{aligned}\tfrac{1}{2}AU^{m,k,[n+1]} + \tfrac{1}{2}M_{-2}U^{m,k,[n+1]}D_m - ZM_{-1}U^{m,k,[n+1]} + NV_\mu U^{m,k,[n+1]} \\ + \sum_{l=0}^{2m_h}(Q_l^{[n]T}\cdot F)(U^{m,k,[n+1]}C^{l,m}) + \sum_{l=0}^{2m_h}V_{\mathrm{xc}}^{l,[n]}U^{m,k,[n+1]}C^{l,m} \\ -\frac{\beta}{\sqrt{3}}M_1U^{m,k,[n+1]}C^{1,m} = \epsilon_{m,k}^{[n+1]}M_0U^{m,k,[n+1]}, \quad (55)\end{aligned}$$

$$\mathrm{Tr}([U^{m,k,[n+1]}]^T M_0 U^{m,k',[n+1]}) = \delta_{kk'}. \quad (56)$$

(3) Build the matrices $R_{l,*}^{[n+1]}$ using the Aufbau principle, and, if necessary, optimizing the occupation numbers $n_{m,k}^{[n+1]}$, by selecting the occupation numbers at the Fermi level leading to the lowest Kohn–Sham energy:[3]

$$R_{l,*}^{[n+1]} = \sum_{\substack{-m_h\le m\le m_h\\ 1\le k\le (m_h-|m|+1)N_h}} n_{m,k}^{[n+1]}U^{m,k,[n+1]}C^{l,m}[U^{m,k,[n+1]}]^T,$$

[3]In practice, this optimization problem is low-dimensional. Indeed, the degeneracy of the Fermi level is typically 3 (perturbation of p-orbitals) or 5 (perturbation of d-orbitals) for most atoms of the first four rows of the periodic table, and some of the occupation numbers are known to be equal for symmetric reasons.

where

$$\begin{cases} n_{m,k}^{[n+1]} = 2 & \text{if } \epsilon_{m,k}^{[n+1]} < \epsilon_{\mathrm{F}}^{[n+1]}, \\ 0 \le n_{m,k}^{[n+1]} \le 2 & \text{if } \epsilon_{m,k}^{[n+1]} = \epsilon_{\mathrm{F}}^{[n+1]}, \\ n_{m,k}^{[n+1]} = 0 & \text{if } \epsilon_{m,k}^{[n+1]} > \epsilon_{\mathrm{F}}^{[n+1]}, \end{cases} \quad \text{and} \quad \sum_{(m,k)} n_{m,k}^{[n+1]} = N.$$

(4) Update the density:

$$\text{for all } 0 \le l \le 2m_h, \quad R_l^{[n+1]} = t_n R_{l,*}^{[n+1]} + (1 - t_n) R_l^{[n]},$$

where $t_n \in [0, 1]$ either is a fixed parameter independent of n and chosen a priori, or is optimized using the optimal damping algorithm (see below).

(5) If (for instance) $\max_{0 \le l \le 2m_h} \| R_l^{[n+1]} - R_l^{[n]} \| \le \epsilon$ or $|E^{[n+1]} - E^{[n]}| \le \varepsilon$, then stop; else go to step (1).

Note that the generalized eigenvalue problem (55)–(56) can be rewritten as a standard generalized eigenvalue problem of the form

$$\mathbb{H}^m \mathbb{V}_k = \epsilon_{m,k}^{[n+1]} \mathbb{M} \mathbb{V}_k, \qquad \mathbb{V}_k^T \mathbb{M} \mathbb{V}_{k'} = \delta_{kk'}, \tag{57}$$

where the unknowns are vectors (and not matrices) by introducing the column vectors $\mathbb{V}_k \in \mathbb{R}^{(m_h+1-|m|)N_h}$ and the block matrices

$$\mathbb{H}^m \in \mathbb{R}^{(m_h+1-|m|)N_h \times (m_h+1-|m|)N_h} \quad \text{and} \quad \mathbb{M} \in \mathbb{R}^{(m_h+1-|m|)N_h \times (m_h+1-|m|)N_h}$$

defined as

$$\mathbb{V}_k = \begin{pmatrix} U_{\cdot,|m|}^{m,k,[n+1]} \\ \hline \vdots \\ \hline U_{\cdot,m_h}^{m,k,[n+1]} \end{pmatrix},$$

$$\mathbb{H}^m = \begin{pmatrix} \mathbb{H}_{|m|,|m|}^m & \mathbb{H}_{|m|,|m|+1}^m & \cdots & \mathbb{H}_{|m|,m_h-1,}^m & \mathbb{H}_{|m|,m_h}^m \\ \hline \mathbb{H}_{|m|+1,|m|}^m & \mathbb{H}_{|m|+1,|m|+1}^m & \cdots & \mathbb{H}_{|m|+1,m_h-1,}^m & \mathbb{H}_{|m|+1,m_h}^m \\ \hline \vdots & \vdots & \ddots & \vdots & \vdots \\ \hline \mathbb{H}_{m_h-1,|m|}^m & \mathbb{H}_{m_h-1,|m|+1}^m & \cdots & \mathbb{H}_{m_h-1,m_h-1,}^m & \mathbb{H}_{m_h-1,m_h}^m \\ \hline \mathbb{H}_{m_h,|m|}^m & \mathbb{H}_{m_h,|m|+1}^m & \cdots & \mathbb{H}_{m_h,m_h-1,}^m & \mathbb{H}_{m_h,m_h}^m \end{pmatrix},$$

and

$$\mathbb{M} = \text{block diag}(M_0, \ldots, M_0),$$

where each of the $(m_h - |m| + 1)$ block $\mathbb{H}^m_{l,l'}$ is of size $N_h \times N_h$ with

for all $|m| \le l \le m_h$,

$$\mathbb{H}^m_{l,l} = \tfrac{1}{2}A + \frac{l(l+1)}{2}M_{-2} - ZM_{-1} + NV_\mu + \sum_{l''=0}^{2m_h} C^{l,m}_{l,l''}([Q^{[n]}_{l''}]^T \cdot F + V^{l'',[n]}_{\mathrm{xc}}),$$

for all $|m| \le l \ne l' \le m_h$,

$$\mathbb{H}^m_{l,l'} = \sum_{l''=0}^{2m_h} C^{l,m}_{l',l''}([Q^{[n]}_{l''}]^T \cdot F + V^{l'',[n]}_{\mathrm{xc}}) - \frac{\beta}{\sqrt{3}} C^{1,m} M_1 \delta_{|l-l'|,1}.$$

If $\beta = 0$ and if the density $\rho^{[n]}_h$ is radial, then $R^{[n]}_l = 0$ for all $l \in \mathbb{N}^*$, and the matrix $\mathbb{H}^m$ is block diagonal. The generalized eigenvalue problem (57) can then be decoupled in $(m_h - |m| + 1)$ independent generalized eigenvalue problems of size N_h. This comes from the fact that, the problem being spherically symmetric, the Kohn–Sham Hamiltonian is block diagonal in the two decompositions

$$L^2(\mathbb{R}^3) = \bigoplus_{l \in \mathbb{N}} \mathscr{H}_l \quad \text{and} \quad L^2(\mathbb{R}^3) = \bigoplus_{m \in \mathbb{Z}} \mathscr{H}^m.$$

Let us conclude this section with some remarks on the optimal damping algorithm (ODA) [5; 6], used to find an optimal step length t_n to mix the matrices $R^{[n+1]}_{l,*}$ and $R^{[n]}_l$ in step (4) of the iterative algorithm. This step length is obtained by minimizing on the range $t \in [0, 1]$ the one-dimensional function

$$t \mapsto \widetilde{E}^{\mathrm{rHF/LDA}}_{Z,N}((1-t)\gamma^{[n+1]}_* + t\gamma^{[n]}, \beta W),$$

where $\gamma^{[n]}$ is the current approximation of the ground state density matrix at iteration n and

$$\gamma^{[n+1]}_* = \sum_{\substack{-m_h \le m \le m_h \\ 1 \le k \le (m_h - |m| + 1)N_h}} n^{[n+1]}_{m,k} |\Phi^{[n+1]}_{m,k,h}\rangle\langle\Phi^{[n+1]}_{m,k,h}|,$$

with

$$\Phi^{[n+1]}_{m,k,h}(r,\theta,\varphi) = \sum_{l=|m|}^{m_h} \sum_{i=1}^{N_h} U^{m,k,[n+1]}_{i,l} \frac{\mathscr{X}_i(r)}{r} Y^m_l(\theta,\varphi).$$

A key observation is that this optimization problem can be solved without storing density matrices, but only the two sets of matrices $R^{[n]} := (R^{[n]}_l)_{0 \le l \le 2m_h}$ and $R^{[n+1]}_* := (R^{[n+1]}_{l,*})_{0 \le l \le 2m_h}$, and the scalars

$$E^{[n]}_{\mathrm{kin}} := \mathrm{Tr}(-\tfrac{1}{2}\Delta\gamma^{[n]})$$

and

$$\begin{aligned} E_{\mathrm{kin},*}^{[n+1]} &:= \mathrm{Tr}(-\tfrac{1}{2}\Delta\gamma_*^{[n+1]}) \\ &= \frac{1}{2} \sum_{\substack{-m_h\le m\le m_h \\ 1\le k\le (m_h-|m|+1)\times N_h}} n_{m,k}^{[n+1]}\big(\mathrm{Tr}([U^{m,k,[n+1]}]^T A U^{m,k,[n+1]}) \\ &\qquad\qquad + \mathrm{Tr}(D_m[U^{m,k,[n+1]}]^T M_{-2} U^{m,k,[n+1]})\big). \end{aligned}$$

Indeed, we have for all $t \in [0, 1]$,

$$\begin{aligned} &\widetilde{E}_{Z,N}^{\mathrm{rHF/LDA}}((1-t)\gamma_*^{[n+1]} + t\gamma^{[n]}, \beta W) \\ &\qquad = (1-t)E_{\mathrm{kin},*}^{[n+1]} + tE_{\mathrm{kin}}^{[n]} + \mathscr{F}^{\mathrm{rHF/LDA}}((1-t)R_*^{[n+1]} + tR^{[n]}, \beta W), \end{aligned}$$

where the functional $\mathscr{F}^{\mathrm{rHF/LDA}}$ collects all the terms of the Kohn–Sham functional depending on the density only. When $E_{\mathrm{xc}} = 0$ (rHF model), the function

$$t \mapsto \widetilde{E}_{Z,N}^{\mathrm{rHF/LDA}}((1-t)\gamma_*^{[n+1]} + t\gamma^{[n]}, \beta W)$$

is a convex polynomial of degree two, and its minimizer on [0, 1] can therefore be easily computed explicitly. In the LDA case, the minimum on [0, 1] of the above function of t can be obtained using any line search method. We use here the golden search method. Once the minimizer t_n is found, the quantity $E_{\mathrm{kin}}^{[n]}$ is updated using the relation

$$E_{\mathrm{kin}}^{[n+1]} = (1-t_n)E_{\mathrm{kin},*}^{[n+1]} + t_n E_{\mathrm{kin}}^{n}.$$

The source code of a Fortran 95 implementation of the method is available on GitHub [27].

4. Numerical results

As previously mentioned, we use in our code, written in Fortran 95 and linked to the BLAS, LAPACK, and ARPACK libraries, the same basis to discretize the radial components of the Kohn–Sham orbitals and of the Hartree potential, that is, $(\mathscr{X}_i)_{1\le i\le N_h} = (\zeta_i)_{1\le i\le N_h}$, and the $\mathbb{P}_4$ finite elements method to construct the discretization basis.

In order to test our methodology on LDA-type models, we have chosen to work with the Xα model [34], which has a simple analytic expression

$$E_{\mathrm{xc}}(\rho) = -\frac{3}{4}\Big(\frac{3}{\pi}\Big)^{1/3}\int_{\mathbb{R}^3}\rho^{4/3} \quad \text{and} \quad v_{\mathrm{xc}}(\rho) = -\Big(\frac{3}{\pi}\Big)^{1/3}\rho^{1/3}.$$

The exchange-correlation contributions must be computed by numerical quadratures. We use here the Gauss quadrature method with $N_{\mathrm{g},r} = 15$ and $N_{\mathrm{g},\theta} = 30$ (see Section 3.1.4).

We start this section by studying the convergence rate of the ground state energy and of the occupied energy levels of the carbon atom ($Z = 6$) as functions of the

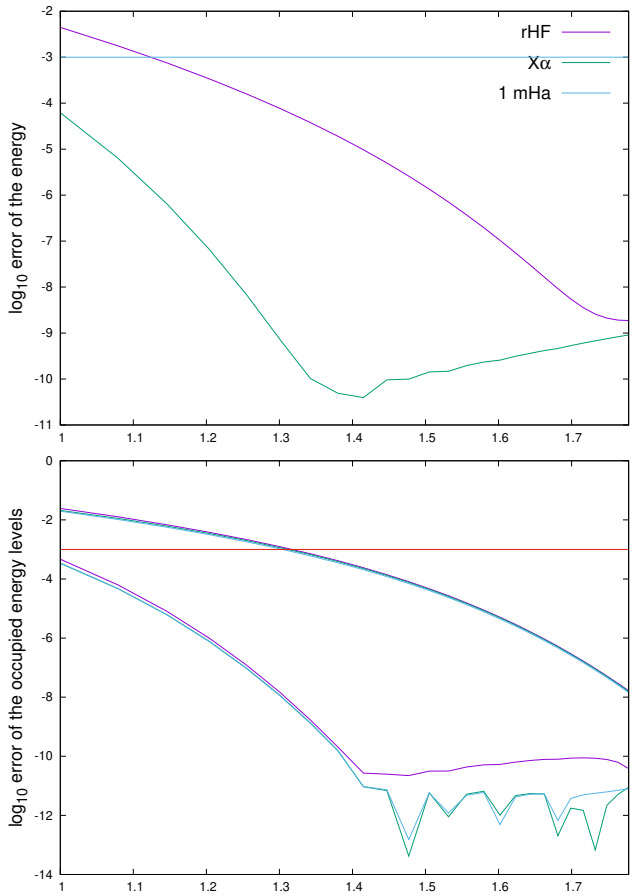

Figure 1. Log-log plot of the error on the total energy (top) and the three occupied energy levels (bottom) of the carbon atom for the rHF (solid lines) and Xα (dashed lines) models as a function of the cut-off radius L_e for a fixed mesh size $N_I = 50$ (the reference calculation corresponds to $L_e = 100$ and $N_I = 100$).

cut-off radius L_e and the mesh size N_I (see Section 3.1.4). The errors on the total energy and on the occupied energy levels for the rHF and Xα models are plotted in Figure 1 (for $L_e = 50$ and different values of N_I) and Figure 2 (for $N_I = 50$ and different values of L_e), the reference calculation corresponding to $L_e = 100$ and $N_I = 100$. We can see that the choice $L_e = 50$ and $N_I = 50$ provides accuracies of about 1 μHa (recall that chemical accuracy corresponds to 1 mHa).

Note that the convergence of the ground state energy and occupied energy levels with respect to the cut-off radius L_e is much faster for Xα than for rHF. This is due to the fact that the energies of the highest occupied orbitals are closer to zero for the rHF model, leading to a slower asymptotic decay at infinity of the ground state

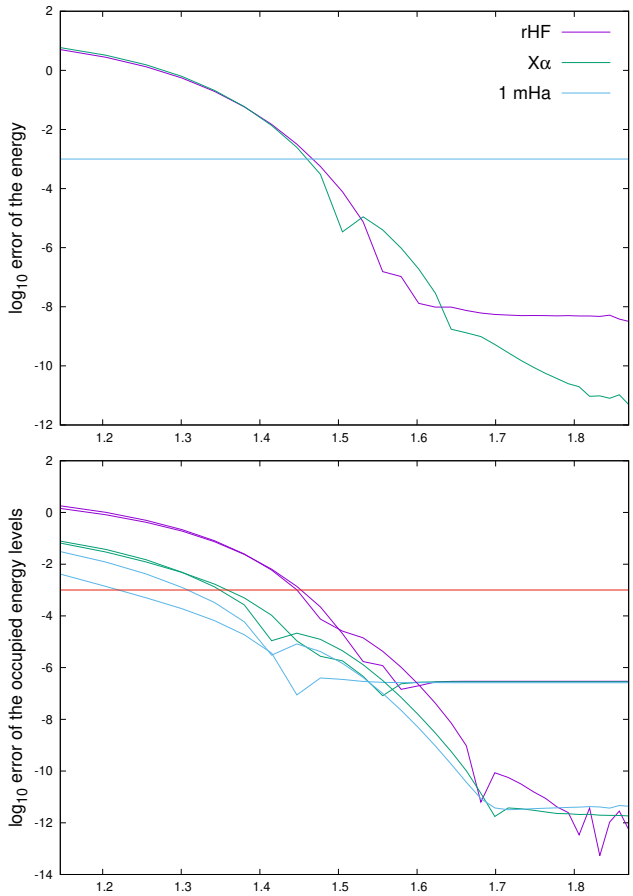

Figure 2. Log-log plot of the error on the total energy (top) and the three occupied energy levels (bottom) of the carbon atom for the rHF (solid lines) and Xα (dashed lines) models as a function of the mesh size N_I, for a fixed cut-off radius $L_e = 50$ (the reference calculation corresponds to $L_e = 100$ and $N_I = 100$).

density. In contrast, the convergence rates with respect to the mesh size are almost the same for the two models.

4.1. ***Electronic structures of isolated atoms.*** We report here calculations on all the atoms of the first four rows of the periodic table obtained with the rHF (Section 4.1.1) and Xα (Section 4.1.2) models.

4.1.1. *Occupied energy levels in the rHF model.* The numerical results presented in this section indicate that, for neutral atoms, the assumption

$$\epsilon^{0,\mathrm{rHF}}_{Z,Z,\mathrm{F}} \text{ is negative and is not an accidentally degenerate eigenvalue of } H^{0,\mathrm{rHF}}_{Z,Z},$$

which guarantees the uniqueness of the nonmagnetic rHF ground state density matrix (Theorem 1), is satisfied for all the chemical elements of the first two rows of the periodic table, and for most of the elements of the third and four rows. Surprisingly, we observe accidental degeneracies at the Fermi level for Sc and Ti (4p and 3d shells), for V, Cr, Mn, and Fe (5s and 3d shells), for Zr (5p and 4d shells), for Nb and Mo (6s and 4d shells), and for Pd and Ag (5s and 4d shells). For some of these elements, the Fermi level is clearly negative, and we can conclude that (see Appendix C)

- if the Fermi level contains an s and a d shell, then the nonmagnetic rHF ground state is unique and
- if the Fermi level contains a p and a d shell, and if both shells are partially occupied (which is suggested by our numerical simulations), then the nonmagnetic rHF ground state is not unique.

For other chemical elements, such as iron ($Z = 26$), the Fermi level is so close to zero that the numerical accuracy of our numerical method does not allow us to know whether it is slightly negative or equal to zero.

The negative eigenvalues of $H_{\rho^0}^{\mathrm{rHF}}$ for all $1 \le Z \le 54$ (first four rows of the periodic table) are listed in Appendix A. The results for $1 \le Z \le 20$, $27 \le Z \le 39$, $43 \le Z \le 45$, and $48 \le Z \le 54$ correspond to N_I increasing from 35 to 75 as Z increases and L_e increasing from 30 to 100 as $|\epsilon_{Z,Z,\mathrm{F}}^{0,\mathrm{rHF}}|$ decreases, which were sufficient to obtain an accuracy of 1 μHa. The remaining atoms are more difficult to deal with because the Fermi level seems to be an accidentally degenerate eigenvalue of $H_{\rho^0}^{\mathrm{rHF}}$ associated with

- the 4p and 3d shells for $Z = 21$ and $Z = 22$,
- the 5s and 3d shells for $23 \le Z \le 26$, with a Fermi level very close (or possibly equal) to zero,
- the 5p and 4d shells for $Z = 40$, with a Fermi level very close (or possibly equal) to zero,
- the 6s and 4d shells for $Z = 41$ and $Z = 42$, with a Fermi level very close (or possibly equal) to zero, and
- the 5s and 4d shells for $Z = 46$ and $Z = 47$.

Since the radial component of the highest occupied orbital typically vanishes as $\exp(-\sqrt{2|\epsilon_{Z,Z,\mathrm{F}}^{0,\mathrm{rHF}}|}r)$ if $\epsilon_{Z,N,\mathrm{F}}^{0,\mathrm{rHF}} < 0$ and algebraically if $\epsilon_{Z,Z,\mathrm{F}}^{0,\mathrm{rHF}} = 0$, a very large value of L_e is needed for the atoms for which the Fermi level is very close or possibly equal to zero. For that case, we use a nonuniform grid with $N_I' = 80$ and $L_e' = 100$ as explained in Section 3.1.4 and glue to it a uniform one with 10 points and length $L_e - L_e'$ varying from 70 to 700. Lastly, we add to the basis a function with an unbounded support, equal to L_e/r on $[L_e, +\infty)$ (see [9] for details). This was sufficient to obtain an accuracy of 10 μHa.

When the accidental degeneracy involves an s shell and since the density is radial, the problem of finding the occupation numbers at the Fermi level reduces to finding a single parameter $t_0 \in [0, 1]$, which encodes the amount of electrons on the upper s shell. In other words, one can write

$$\rho_{Z,Z}^{0,\mathrm{rHF}} = \rho_{\mathrm{f}} + t_0 \rho_{\mathrm{s}} + (1 - t_0)\rho_{\mathrm{d}},$$

where ρ_{f} is the density corresponding to the fully occupied shells, and where ρ_{s} and ρ_{d} are densities corresponding to the accidentally degenerate s and d shells. Using the same trick for accidentally degenerate p and d shells, we manage to obtain a self-consistent solution to the rHF equations, which is necessarily a ground state since the rHF model is convex in the density matrix.

In the following tables, we report the rHF occupied energy levels (in Ha) of all the atoms of the first four rows of the periodic table, for which the Fermi level seems to be an accidentally degenerate eigenvalue:

- the 4p and 3d orbitals have the same energy for $Z = 21, 22$,
- the 5s and 3d orbitals have the same energy for $23 \leq Z \leq 26$,
- the 5p and 4d orbitals have the same energy for $Z = 40$,
- the 6s and 4d orbitals have the same energy for $Z = 41, 42$, and
- the 5s and 4d orbitals have the same energy for $Z = 46, 47$.

In all these cases, the occupation number $0 \leq n \leq 2$ of the partially occupied d orbitals is also given.

Third row.

Atom	Sc	Ti	V	Cr	Mn	Fe
Z	21	22	23	24	25	26
1s	−154.35864	−171.13186	−188.77080	−207.27457	−226.64207	−246.87446
2s	−15.78538	−17.95490	−20.24077	−22.64280	−25.15938	−27.79250
2p	−12.74151	−14.69008	−16.75392	−18.93275	−21.22503	−23.63263
3s	−1.69002	−1.91684	−2.15109	−2.39225	−2.63884	−2.89238
3p	−0.96964	−1.11529	−1.26708	−1.42402	−1.58451	−1.74975
4s	−0.08646	−0.08224	−0.07796	−0.07027	−0.06385	−0.05831
4p	−0.00262	−0.00056				
5s			−0.00044	−0.00021	−0.00008	−0.00001
3d	−0.00262	−0.00056	−0.00044	−0.00021	−0.00008	−0.00001
n (3d)	0.0056	0.3076	0.5662	0.7794	0.9886	1.1957

Fourth row.

Atom	Zr	Nb	Mo	Pd	Ag
Z	40	41	42	46	47
1s	−627.17364	−661.38533	−696.51265	−846.21733	−885.91821
2s	−83.77963	−89.25420	−94.89727	−119.19036	−125.66905
2p	−76.25111	−81.47185	−86.85999	−110.12295	−116.34159
3s	−12.93681	−14.14588	−15.39104	−20.77177	−22.19282
3p	−10.23529	−11.31538	−12.43032	−17.27895	−18.56438
3d	−5.37710	−6.20667	−7.06960	−10.89439	−11.91967
4s	−1.58204	−1.76423	−1.94236	−2.66438	−2.82492
4p	−0.89248	−1.01284	−1.13016	−1.61336	−1.71460
5s	−0.07367	−0.06267	−0.04957	−0.03846	−0.03379
5p	−0.00048				
6s		−0.00014	−0.000002		
4d	−0.00048	−0.00014	−0.000002	−0.03846	−0.03379
n (4d)	0.3207	0.5840	0.7983	1.6655	1.9293

The occupied energy levels in the rHF model of all the atoms of the first four rows of the periodic table are given in Appendix A.

Remark. Our numerical simulations seem to show that for all $1 \leq Z \leq 54$, there are no unoccupied negative eigenvalues in the rHF ground states of neutral atoms. Thus, the negative spectrum of the rHF Hamiltonian coincides with the set of occupied energy levels.

We end this section with Figure 3, which backs up the conjecture that rHF atomic densities are decreasing radial functions of the distance to the nucleus.

4.1.2. *Occupied energy levels in the* Xα *model.* The tables below provide the negative eigenvalues of the Kohn–Sham Xα Hamiltonian (in Ha) for all the atoms of the first four rows of the periodic table with accidentally degenerate Fermi levels, the degeneracy occurring in all cases between an s shell and a d shell (4s–3d for $23 \leq Z \leq 28$, 5s–4d for $41 \leq Z \leq 44$). All the results of this section are obtained for $L_e = 30$ and N_I increasing from 30 to 75 as Z increases.

Third row.

Atom	V	Cr	Mn	Fe	Co	Ni
Z	23	24	25	26	27	28
1s	−195.11079	−213.87746	−233.50875	−254.00470	−275.36535	−297.59075
2s	−21.72028	−24.14440	−26.68762	−29.35014	−32.13212	−35.03372
2p	−18.33888	−20.55424	−22.88690	−25.33699	−27.90468	−30.59009
3s	−2.44810	−2.68033	−2.92165	−3.17214	−3.43191	−3.70102
3p	−1.53340	−1.68342	−1.83995	−2.00304	−2.17274	−2.34907
4s	−0.13684	−0.13575	−0.13474	−0.13379	−0.13292	−0.13212
3d	−0.13684	−0.13575	−0.13474	−0.13379	−0.13292	−0.13212
n (3d)	0.6393	0.8873	1.1278	1.3622	1.5918	1.8174

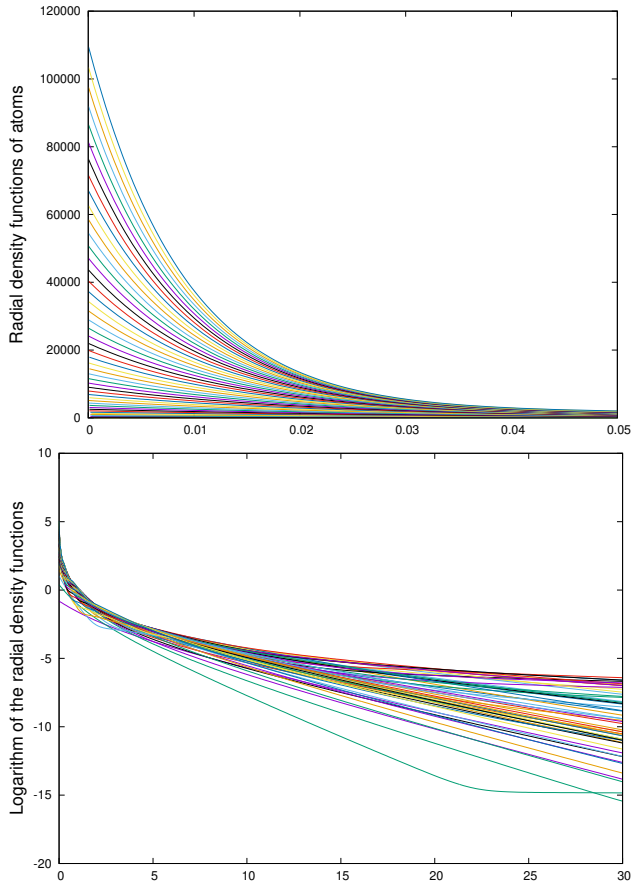

Figure 3. Top: the plot of the densities of all the atoms $1 \leq Z \leq 54$ obtained with our code as a function of the distance to the nucleus, on the interval [0, 0.05]. Bottom: the plot of the logarithms of those densities on the interval [0, 50].

Fourth row.

Atom	Nb	Mo	Tc	Ru
Z	41	42	43	44
1s	−673.74149	−709.15136	−745.48044	−782.72787
2s	−92.74707	−98.44597	−104.31826	−110.36286
2p	−85.27606	−90.73190	−96.35989	−102.15896
3s	−15.40918	−16.63439	−17.90004	−19.20531
3p	−12.56830	−13.66757	−14.80629	−15.98365
3d	−7.35588	−8.21062	−9.10349	−10.03361
4s	−2.05942	−2.19877	−2.34006	−2.48279
4p	−1.27048	−1.35425	−1.43939	−1.52544
5s	−0.13172	−0.11937	−0.10617	−0.09183
4d	−0.13172	−0.11937	−0.10617	−0.09183
n (4d)	0.6535	0.9847	1.2956	1.5896

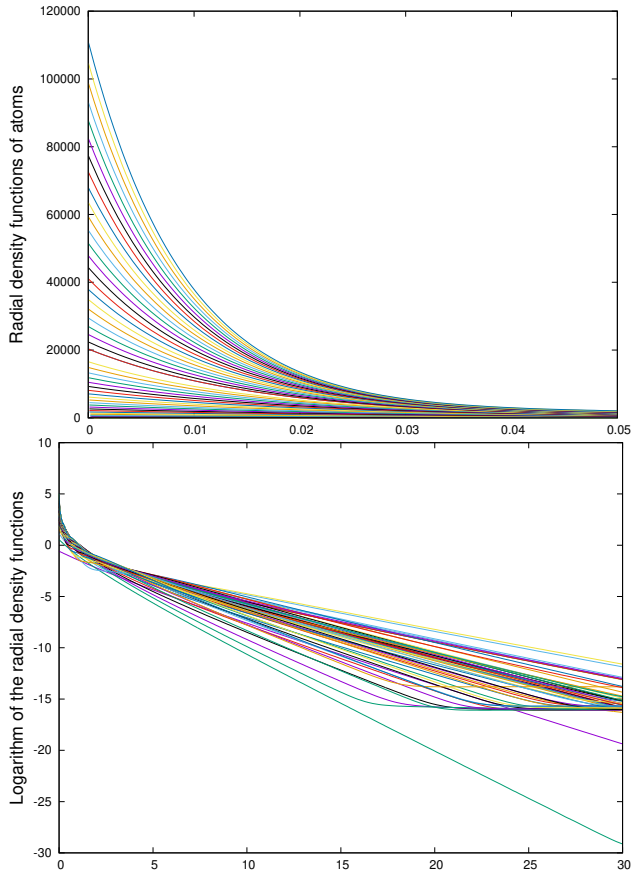

Figure 4. Top: the plot of the Xα densities of all the atoms $1 \leq Z \leq 54$ obtained with our code as a function of the distance to the nucleus, on the interval [0, 0.05]. Bottom: the plot of the logarithms of those densities on the interval [0, 50].

The occupied energy levels in the Xα model of all the atoms of the first four rows of the periodic table are given in Appendix B.

We end this section with Figure 4, which shows that as in the rHF case, the Xα atomic densities seem to be decreasing radial functions of the distance to the nucleus.

4.2. ***Perturbation by a uniform electric field*** **(*Stark effect*).** In this section, we consider atoms subjected to a uniform electric field, that is, to an external potential βW_{Stark} with

$$W_{\text{Stark}}(\boldsymbol{r}) = -e_z \cdot \boldsymbol{r}$$

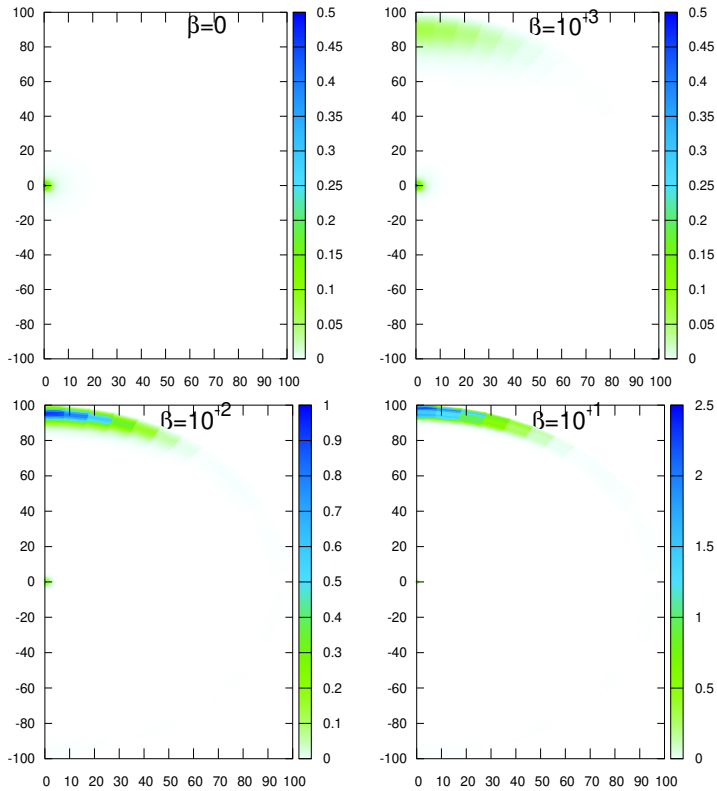

Figure 5. rHF case: at the top left is a plot in the ϱz-half-plane of the ground state density (multiplied by r^2) of an isolated carbon atom. The others are plots of the ground state densities (multiplied by r^2) of the carbon atom in a sphere of radius $L_e = 100$, subjected to a uniform external electric field, with coupling constants $\beta = 10^{-3}, 10^{-2}, 10^{-1}$.

or, in spherical coordinates,

$$W_{\text{Stark}}(r, \theta, \varphi) = -\sqrt{\frac{4\pi}{3}}\, r\, Y_1^0(\theta, \varphi).$$

As already mentioned in Section 2.2, $\widetilde{\mathcal{F}}_{Z,N}^{\text{rHF/LDA}}(\beta W_{\text{Stark}}) = -\infty$ whenever $\beta \neq 0$, and the corresponding variational problem has no minimizer. However, one can find a minimizer $\gamma_h \in \mathcal{K}_{N,h}$ to the approximated problem $\widetilde{\mathcal{F}}_{Z,N,h}^{\text{rHF/LDA}}(\beta W_{\text{Stark}})$. Hereafter we consider the carbon atom ($Z = 6$). Even though the cutoff m_h is set equal to 6, all the terms corresponding to a magnetic number $m > 1$ are in fact equal to zero.

Recall that the perturbed ground state density is cylindrically symmetric about the z-axis. Figures 5 and 6 are plots in the ϱz-half-plane ($\varrho = r \sin\theta$ and $z = r\cos\theta$) of the densities ρ_h (multiplied by r^2 in order to emphasize what is going on at large distances from the nucleus), for the carbon atom ($Z = 6$), obtained for different values of β.

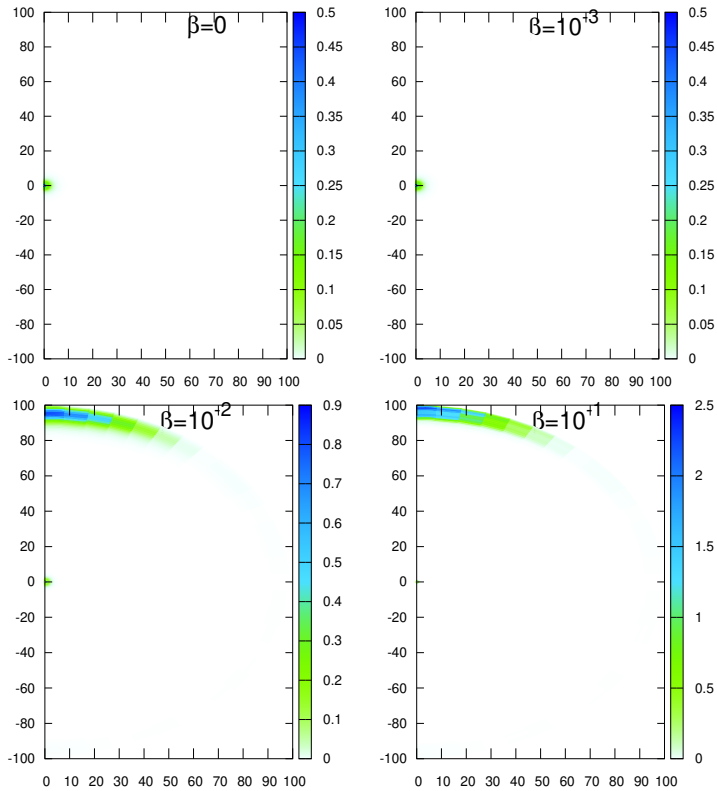

Figure 6. Xα case: at the top left is a plot in the ϱz-half-plane of the ground state density (multiplied by r^2) of an isolated carbon atom. The others are plots of the ground state densities (multiplied by r^2) of the carbon atom in a sphere of radius $L_e = 100$, subjected to a uniform external electric field, with coupling constants $\beta = 10^{-3}, 10^{-2}, 10^{-1}$.

For $\beta = 10^{-2}$ and $\beta = 10^{-1}$, we clearly see spurious boundary effects: part of the electronic cloud is localized in the region where the external potential takes highly negative values. This result is obviously not physical. On the other hand, for the Xα model and for $\beta = 10^{-3}$ we simply observe a polarization of the electronic cloud. The perturbation potential being not spherically symmetric, it breaks the symmetry of the density. This numerical solution can probably be interpreted as a (nonlinear) resonant state. We will come back to the analysis of this interesting case in a following work.

Figure 7 shows the amount of electrons of the carbon atom which escape to infinity as a function of the coupling constant β (for $L_e = 100$ and $N_I = 50$), in the rHF and Xα cases.

In general, the standard ODA is used to achieve convergence (see Section 3). However, for β small or large enough, the occupation numbers are selected as follows: $n_{0,1}^{[n]} = n_{0,2}^{[n]} = 2$, $n_{0,3} = 2(1 - t_0)$, and $n_{1,1}^{[n]} = 2 - n_{0,3} = 2t_0$, t_0 being the

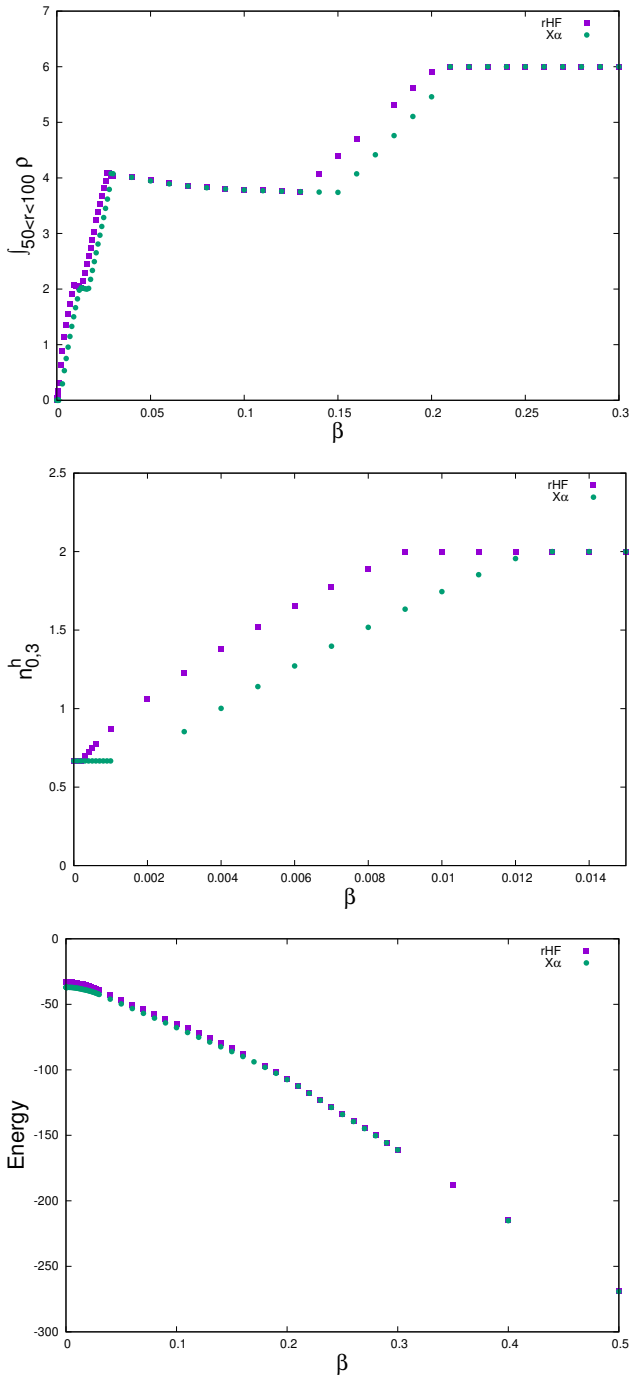

Figure 7. Top: the plot of the integral on $B_{100} \setminus B_{50}$ of the density ρ_h. Middle: the plot of the occupation number $n^h_{0,3}$. Bottom: the plot of the total energy, for $L_e = 100$ and $N_I = 50$ as a function of β in the rHF and Xα cases.

minimizer of

$$t \mapsto \widetilde{E}_{6,6}^{\mathrm{rHF/LDA}}((1-t)\gamma_{0,*}^{[n]} + t\gamma_{1,*}^{[n]}, \beta W),$$

where

$$\gamma_{0,*}^{[n]} = 2\sum_{1\le k\le 3} |\Phi_{0,k,h}\rangle\langle\Phi_{0,k,h}|, \quad \gamma_{1,*}^{[n]} = 2\sum_{1\le k\le 2} |\Phi_{0,k,h}\rangle\langle\Phi_{0,k,h}| + 2|\Phi_{1,1,h}\rangle\langle\Phi_{1,1,h}|.$$

This modification of ODA significantly increases the rate of convergence for β small or large, but does not converge for all intermediate values of β.

While $\widetilde{\mathcal{I}}_{Z,N}^{\mathrm{rHF/LDA}}(\beta W_{\mathrm{Stark}}) = -\infty$ and the corresponding variational problem has no minimizer, the first-order perturbation $\gamma_{Z,N,W_{\mathrm{Stark}}}^{(1),\mathrm{rHF}}$ of the ground state density matrix does exist (see Theorem 4). If we consider the carbon atom, it can be expressed as a function of the unperturbed occupied Kohn–Sham orbitals and of their first-order perturbations. We indeed have

$$\gamma_{6,6,W_{\mathrm{Stark}}}^{(1),\mathrm{rHF}} = \sum_{\substack{(m,k)\in\mathbb{O}_{6,6}\\ i_1\ge 0,\, i_2\ge 0,\, i_3\ge 0\\ i_1+i_2+i_3=1}} n_{m,k}^{(i_1)} |\Phi_{m,k}^{(i_2)}\rangle\langle\Phi_{m,k}^{(i_3)}|,$$

where $\mathbb{O}_{6,6} = \{(0,1), (0,2), (0,3), (1,1)\}$, where $\epsilon_{m,k}^{(0)}$ is the k-th lowest eigenvalue of $H_{6,6}^{0,\mathrm{rHF}}$ in the subspace $\mathcal{H}^m$, $\Phi_{m,k}^{(0)}$ is an associated normalized eigenfunction, and

$$n_{0,1}^{(0)} = n_{0,2}^{(0)} = 2, \quad n_{0,3}^{(0)} = \tfrac{2}{3}, \quad \text{and} \quad n_{1,1}^{(0)} = \tfrac{4}{3},$$

while $\epsilon_{m,k}^{(1)}$, $\Phi_{m,k}^{(1)}$, and $n_{m,k}^{(1)}$ satisfy the self-consistent equation

$$\begin{gathered}
(H_{6,6}^{0,\mathrm{rHF}} - \epsilon_{m,k}^{(0)})\Phi_{m,k}^{(1)} + (\rho^{(1)} \star |\cdot|^{-1})\Phi_{m,k}^{(0)} + W_{\mathrm{Stark}}\Phi_{m,k}^{(0)} = \epsilon_{m,k}^{(1)}\Phi_{m,k}^{(0)},\\
\rho^{(1)} = \sum_{(m,k)\in\mathbb{O}_{6,6}} 2\, n_{m,k}^{(0)}\Phi_{m,k}^{(0)}\Phi_{m,k}^{(1)} + n_{m,k}^{(1)}\Phi_{m,k}^{(0)}\Phi_{m,k}^{(0)},\\
\int_{\mathbb{R}^3} \Phi_{m,k}^{(1)}\Phi_{m,k}^{(0)} = 0, \quad \text{and} \quad \sum_{(m,k)\in\mathbb{O}_{6,6}} n_{m,k}^{(1)} = 0.
\end{gathered}$$

We denote by $\epsilon_{m,k,h}^{(0)}$, $\epsilon_{m,k,h}^{(1)}$, $\Phi_{m,k,h}^{(0)}$, $\Phi_{m,k,h}^{(1)}$, and $n_{m,k,h}^{(1)}$ the approximations of $\epsilon_{m,k}^{(0)}$, $\epsilon_{m,k}^{(1)}$, $\Phi_{m,k}^{(0)}$, $\Phi_{m,k}^{(1)}$, and $n_{m,k}^{(1)}$, respectively. For each $(m,k) \in \mathbb{O}_{6,6}$, define

$$\begin{aligned}
\widetilde{\epsilon}_{m,k,h}^{(1)}(\beta) &:= \frac{1}{\beta}(\epsilon_{m,k,h}(\beta) - \epsilon_{m,k,h}^{(0)}),\\
\widetilde{\Phi}_{m,k,h}^{(1)}(\beta) &:= \frac{1}{\beta}(\Phi_{m,k,h}(\beta) - \Phi_{m,k,h}^{(0)}),\\
\widetilde{n}_{m,k,h}^{(1)}(\beta) &:= \frac{1}{\beta}(n_{m,k,h}(\beta) - n_{m,k}^{(0)}).
\end{aligned}$$

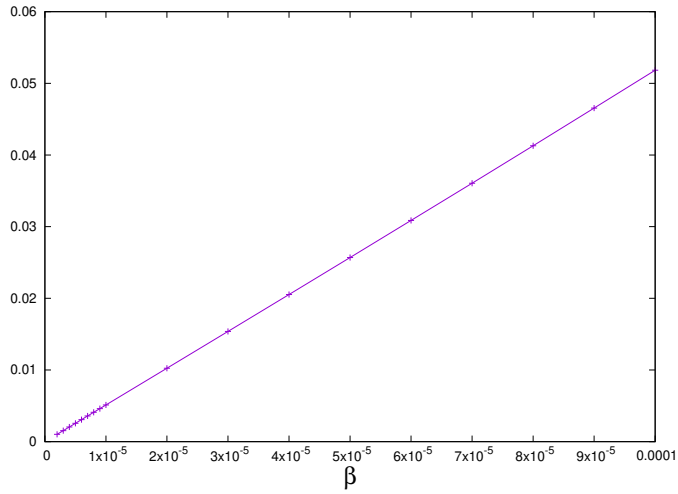

Figure 8. Plot of the function $\beta \mapsto \max_{(m,k)|n_{m,k}>0} \max_{l\geq|m|} \|V_{l,(m,k)}(\beta)\|_\infty$ where $V_{l,(m,k)}(\beta)$ is the vector in the left-hand side of (58).

Recall that $(\Phi_{m,k,h}(\beta))_{(m,k)\in\mathbb{C}_{6,6}}$ and $n^{(1)}_{m,k,h}(\beta)$ are the eigenfunctions and eigenvalues, respectively, of the density matrix γ_h, the minimizer of the approximated problem $\widetilde{\mathcal{F}}^{\mathrm{rHF}}_{Z,N,h}(\beta W_{\mathrm{Stark}})$.

Let $U^{m,k}$ and $\widetilde{U}^{m,k}(\beta)$ be such that

$$\Phi^{(0)}_{m,k,h}(r,\theta,\varphi) = \sum_{l=|m|}^{m_h}\left(\sum_{i=1}^{N_h} U^{m,k}_{i,l}(\beta)\mathscr{X}_i(r)/r\right)Y^m_l(\theta,\varphi),$$

$$\widetilde{\Phi}^{(1)}_{m,k,h}(\beta)(r,\theta,\varphi) = \sum_{l=|m|}^{m_h}\left(\sum_{i=1}^{N_h} \widetilde{U}^{m,k}_{i,l}(\beta)\mathscr{X}_i(r)/r\right)Y^m_l(\theta,\varphi).$$

To show that $\widetilde{\Phi}^{(1)}_{m,k,h}(\beta) \to \Phi^{(1)}_{m,k,h}$ when $\beta \to 0$, it is enough to show that for each $l \geq 0$

$$\begin{aligned}\left(\tfrac{1}{2}A + \frac{l(l+1)}{2}M_{-2} - ZM_{-1} + NV_\mu - \epsilon^{(0)}M_0\right)\widetilde{U}_{\cdot,l}(\beta) - \frac{1}{\sqrt{3}}C^{1,m}M_1U_{\cdot,l-1}\\ - \frac{1}{\sqrt{3}}C^{1,m}M_1U_{\cdot,l+1} + \sum_{l'=|m|}^{m_h}\sum_{l''=0}^{2m_h} C^{l,m}_{l',l''}([Q_{l''}]^T\cdot F)\widetilde{U}_{\cdot,l'}(\beta)\\ + C^{l,m}_{l',l''}([\widetilde{Q}_{l''}(\beta)]^T\cdot F)U_{\cdot,l'} - \epsilon^{(1)}M_0U_{\cdot,l} \underset{\beta\to 0}{\to} 0. \qquad (58)\end{aligned}$$

The index (m,k) is omitted for simplicity, and the vector $\widetilde{Q}_l(\beta)$ is the solution to the linear system

$$(A^{\mathrm{a}} + l(l+1)M^{\mathrm{a}}_{-2})\widetilde{Q}_l = 4\pi F : \widetilde{R}_l,$$

with

$$\widetilde{R}_l := \sum_{\substack{-m_h \le m \le m_h \\ 1 \le k \le (m_h - |m| + 1) \times N_h}} 2n^{(0)}_{m,k} \widetilde{U}^{m,k} C^{l,m} [\widetilde{U}^{m,k}]^T + n^{(1)}_{m,k} \widetilde{U}^{m,k} C^{l,m} [U^{m,k}]^T .$$

Our numerical results show that, as expected by symmetry, $n^{(1)}_{m,k,h} = \epsilon^{(1)}_{m,k,h} = 0$ for all $(m, k) \in \mathbb{O}_{6,6}$, and that the left-hand side of (58) converges to zero linearly in β (see Figure 8).

Appendix A: Occupied energy levels in the rHF model

In the following tables, we report the rHF occupied energy levels (in Ha) of all the atoms of the first four rows of the periodic table. In case the Fermi level seems to be an accidentally degenerate eigenvalue, the occupation number $0 \le n \le 2$ of the partially occupied d orbitals is also given.

Hydrogen and helium.

Atom	Z	1s
H	1	−0.046222
He	2	−0.184889

First row.

Atom	Z	1s	2s	2p
Li	3	−1.202701	−0.013221	
Be	4	−2.902437	−0.043722	
B	5	−5.407212	−0.164961	−0.002389
C	6	−8.555732	−0.265682	−0.012046
N	7	−12.390177	−0.384699	−0.027312
O	8	−16.912538	−0.522883	−0.047280
F	9	−22.123525	−0.680479	−0.071663
Ne	10	−28.023481	−0.857597	−0.100342

Second row.

Atom	Z	1s	2s	2p	3s	3p
Na	11	−35.065314	−1.453872	−0.514340	−0.012474	
Mg	12	−42.963178	−2.169348	−1.037891	−0.034036	
Al	13	−51.833760	−3.118983	−1.789953	−0.135543	−0.002486
Si	14	−61.532179	−4.160128	−2.629056	−0.208803	−0.010768
P	15	−72.083951	−5.319528	−3.582422	−0.284199	−0.023431
S	16	−83.489746	−6.598489	−4.651551	−0.363585	−0.039746
Cl	17	−95.749535	−7.997404	−5.836930	−0.447628	−0.059401
Ar	18	−108.863191	−9.516434	−7.138772	−0.536669	−0.082233

Third row.

Atom	K	Ca	Sc	Ti
Z	19	20	21	22
1s	−123.093717	−138.233855	−154.35864	−171.13186
2s	−11.413369	−13.478564	−15.78538	−17.95490
2p	−8.815789	−10.658837	−12.74151	−14.69008
3s	−0.866180	−1.225936	−1.69002	−1.91684
3p	−0.326113	−0.596554	−0.96964	−1.11529
4s	−0.009500	−0.024275	−0.08646	−0.08224
4p			−0.00262	−0.00056
3d			−0.00262	−0.00056
n (3d)			0.0056	0.3076

Atom	V	Cr	Mn	Fe
Z	23	24	25	26
1s	−188.77080	−207.27457	−226.64207	−246.87446
2s	−20.24077	−22.64280	−25.15938	−27.79250
2p	−16.75392	−18.93275	−21.22503	−23.63263
3s	−2.15109	−2.39225	−2.63884	−2.89238
3p	−1.26708	−1.42402	−1.58451	−1.74975
4s	−0.07796	−0.07027	−0.06385	−0.05831
5s	−0.00044	−0.00021	−0.00008	−0.00001
3d	−0.00044	−0.00021	−0.00008	−0.00001
n (3d)	0.5662	0.7794	0.9886	1.1957

Atom	Co	Ni	Cu	Zn
Z	27	28	29	30
1s	−267.97363	−289.94364	−312.78019	−336.48301
2s	−30.54468	−33.42047	−36.41574	−39.53045
2p	−26.15798	−28.80557	−31.57124	−34.45491
3s	−3.15502	−3.43107	−3.71624	−4.01038
3p	−1.92172	−2.10456	−2.29392	−2.48957
4s	−0.05438	−0.05459	−0.05539	−0.05646
3d	−0.00121	−0.00722	−0.01370	−0.02026

Atom	Ga	Ge	As	Se	Br	Kr
Z	31	32	33	33	35	36
1s	−361.309461	−387.039855	−413.704397	−441.297733	−469.815876	−499.256211
2s	−43.037010	−46.711685	−50.583856	−54.647174	−58.896767	−63.329305
2p	−37.727020	−41.164308	−44.796323	−48.616891	−52.621294	−56.806329
3s	−4.576035	−5.182760	−5.856750	−6.590128	−7.377307	−8.214637
3p	−2.951273	−3.449483	−4.011096	−4.628856	−5.297678	−6.014298
3d	−0.264266	−0.533749	−0.860725	−1.240224	−1.668313	−2.142323
4s	−0.165288	−0.229337	−0.293291	−0.358794	−0.426192	−0.495638
4p	−0.002386	−0.010542	−0.022574	−0.037413	−0.054625	−0.073991

Fourth row.

Atom	Rb	Sr	Y	Zr	Nb	Mo
Z	37	38	39	40	41	42
1s	−529.827018	−561.340511	−593.866153	−627.17364	−661.38533	−696.51265
2s	−68.150675	−73.171957	−78.461974	−83.77963	−89.25420	−94.89727
2p	−61.378353	−66.148672	−71.186183	−76.25111	−81.47185	−86.85999
3s	−9.306434	−10.462839	−11.752114	−12.93681	−14.14588	−15.39104
3p	−6.983328	−8.015158	−9.178245	−10.23529	−11.31538	−12.43032
3d	−2.867015	−3.653051	−4.569112	−5.37710	−6.20667	−7.06960
4s	−0.760103	−1.032665	−1.383317	−1.58204	−1.76423	−1.94236
4p	−0.271916	−0.475893	−0.757307	−0.89248	−1.01284	−1.13016
5s	−0.008742	−0.021586	−0.076589	−0.07367	−0.06267	−0.04957
5p			−0.002707	−0.00048		
6s					−0.00014	−0.000002
4d				−0.00048	−0.00014	−0.000002
n (4d)				0.3207	0.5840	0.7983

Atom	Tc	Ru	Rh	Pd	Ag
Z	43	44	45	46	47
1s	−732.565071	−769.539351	−807.43252	−846.21733	−885.91821
2s	−100.718115	−106.713582	−112.88067	−119.19036	−125.66905
2p	−92.424856	−98.163269	−104.07224	−110.12295	−116.34159
3s	−16.681758	−18.014957	−19.3877	−20.77177	−22.19282
3p	−13.589644	−14.790336	−16.02956	−17.27895	−18.56438
3d	−7.975384	−8.920979	−9.90351	−10.89439	−11.91967
4s	−2.126544	−2.314092	−2.50245	−2.66438	−2.82492
4p	−1.254159	−1.381847	−1.51046	−1.61336	−1.71460
5s	−0.044554	−0.043203	−0.04269	−0.03846	−0.03379
4d	−0.009444	−0.024185	−0.04081	−0.03846	−0.03379
n (4d)				1.6655	1.9293

Atom	Cd	In	Sn	Sb
Z	48	49	50	51
1s	−926.623485	−968.415517	−1011.130388	−1054.799726
2s	−132.409803	−139.493172	−146.755434	−154.228103
2p	−122.820764	−129.641175	−136.639081	−143.846051
3s	−23.742846	−25.501835	−27.305190	−29.184036
3p	−19.977847	−21.599353	−23.264351	−25.004010
3d	−13.071777	−14.430695	−15.832028	−17.307019
4s	−3.073669	−3.487846	−3.900956	−4.343505
4p	−1.901671	−2.251916	−2.599067	−2.973930
4d	−0.096713	−0.310885	−0.517562	−0.749756
5s	−0.042861	−0.131665	−0.181855	−0.230820
5p		−0.002570	−0.010599	−0.021622

Atom	Te	I	Xe
Z	52	53	54
1s	−1099.421697	−1144.994552	−1191.517037
2s	−161.909103	−169.796463	−177.888737
2p	−151.260063	−158.879194	−166.702039
3s	−31.136080	−33.159211	−35.251891
3p	−26.816070	−28.698453	−30.649647
3d	−18.853453	−20.469283	−22.153023
4s	−4.812921	−5.307002	−5.824212
4p	−3.374212	−3.797932	−4.243727
4d	−1.006149	−1.285246	−1.585928
5s	−0.280095	−0.330100	−0.381026
5p	−0.034651	−0.049319	−0.065446

Appendix B: Occupied energy levels in the Xα model

The tables below provide the negative eigenvalues of the Kohn–Sham Xα Hamiltonian (in Ha) for all the atoms of the first four rows of the periodic table. We observe that atoms Z, with $23 \leq Z \leq 28$ and $41 \leq Z \leq 44$, have accidentally degenerate Fermi levels, the degeneracy occurring in all cases between an s shell and a d shell (4s–3d for $23 \leq Z \leq 28$ and 5s–4d for $41 \leq Z \leq 44$). All the results of this section are obtained for $L_e = 30$ and N_I increasing from 30 to 75 as Z increases.

Hydrogen and helium.

Atom	Z	1s
H	1	−0.194250
He	2	−0.516968

First row.

Atom	Z	1s	2s	2p
Li	3	−1.820596	−0.079032	−0.019804
Be	4	−3.793182	−0.170028	−0.045681
B	5	−6.502185	−0.305377	−0.100041
C	6	−9.884111	−0.457382	−0.157952
N	7	−13.946008	−0.628841	−0.221004
O	8	−18.690815	−0.820599	−0.289512
F	9	−24.120075	−1.032963	−0.363534
Ne	10	−30.234733	−1.266049	−0.443056

Second row.

Atom	Z	1s	2s	2p	3s	3p
Na	11	−37.647581	−2.007737	−1.006028	−0.077016	
Mg	12	−45.897000	−2.845567	−1.661300	−0.142129	
Al	13	−55.080562	−3.877978	−2.507293	−0.251340	−0.071775
Si	14	−65.107293	−5.017013	−3.456703	−0.359121	−0.117813
P	15	−75.982880	−6.269749	−4.516571	−0.470070	−0.166674
S	16	−87.709076	−7.638741	−5.689399	−0.585627	−0.218875
Cl	17	−100.286615	−9.125221	−6.976378	−0.706438	−0.274567
Ar	18	−113.715864	−10.729883	−8.378170	−0.832845	−0.333798

Third row.

Atom	K	Ca	Sc	Ti
Z	19	20	21	22
1s	−128.330888	−143.848557	−160.10133	−177.19446
2s	−12.775422	−14.981138	−17.14580	−19.39840
2p	−10.219106	−12.218289	−14.17782	−16.22419
3s	−1.233137	−1.655845	−1.94114	−2.21070
3p	−0.646636	−0.981391	−1.18677	−1.37630
4s	−0.064460	−0.111359	−0.12562	−0.13516
3d			−0.08993	−0.12742

Atom	V	Cr	Mn	Fe	Co	Ni
Z	23	24	25	26	27	28
1s	−195.11079	−213.87746	−233.50875	−254.00470	−275.36535	−297.59075
2s	−21.72028	−24.14440	−26.68762	−29.35014	−32.13212	−35.03372
2p	−18.33888	−20.55424	−22.88690	−25.33699	−27.90468	−30.59009
3s	−2.44810	−2.68033	−2.92165	−3.17214	−3.43191	−3.70102
3p	−1.53340	−1.68342	−1.83995	−2.00304	−2.17274	−2.34907
4s	−0.13684	−0.13575	−0.13474	−0.13379	−0.13292	−0.13212
3d	−0.13684	−0.13575	−0.13474	−0.13379	−0.13292	−0.13212
n (3d)	0.6393	0.8873	1.1278	1.3622	1.5918	1.8174

Atom	Cu	Zn	Ga	Ge
Z	29	30	31	32
1s	−320.711183	−344.885966	−370.087065	−396.206872
2s	−38.088382	−41.471174	−45.140343	−48.991790
2p	−33.426318	−36.586685	−40.030943	−43.654803
3s	−4.010749	−4.519851	−5.188704	−5.906101
3p	−2.562693	−2.969457	−3.532081	−4.139819
3d	−0.157720	−0.348234	−0.685727	−1.064181
4s	−0.138533	−0.185366	−0.290872	−0.386783
4p			−0.070624	−0.114696

Atom	As	Se	Br	Kr
Z	33	34	35	36
1s	−423.248196	−451.209748	−480.090322	−509.889039
2s	−53.026929	−57.243491	−61.639549	−66.213681
2p	−47.459904	−51.444139	−55.605706	−59.943283
3s	−6.673183	−7.487710	−8.347907	−9.252538
3p	−4.794502	−5.494354	−6.237921	−7.024197
3d	−1.487148	−1.953579	−2.462342	−3.012574
4s	−0.481338	−0.576513	−0.673116	−0.771572
4p	−0.158885	−0.20426	−0.251199	−0.299874

Fourth row.

Atom	Rb	Sr	Y	Zr
Z	37	38	39	40
1s	−540.863861	−572.774871	−605.539841	−639.200123
2s	−71.219637	−76.418197	−81.718973	−87.167101
2p	−64.711316	−69.670502	−74.731216	−79.938205
3s	−10.452293	−11.708284	−12.932519	−14.171025
3p	−8.104015	−9.238678	−10.340292	−11.455022
3d	−3.854833	−4.750868	−5.612293	−6.485549
4s	−1.088064	−1.407019	−1.651693	−1.873159
4p	−0.547366	−0.798079	−0.980422	−1.141874
5s	−0.061487	−0.102737	−0.120721	−0.131037
4d			−0.071919	−0.111534

Atom	Nb	Mo	Tc	Ru
Z	41	42	43	44
1s	−673.74149	−709.15136	−745.48044	−782.72787
2s	−92.74707	−98.44597	−104.31826	−110.36286
2p	−85.27606	−90.73190	−96.35989	−102.15896
3s	−15.40918	−16.63439	−17.90004	−19.20531
3p	−12.56830	−13.66757	−14.80629	−15.98365
3d	−7.35588	−8.21062	−9.10349	−10.03361
4s	−2.05942	−2.19877	−2.34006	−2.48279
4p	−1.27048	−1.35425	−1.43939	−1.52544
5s	−0.13172	−0.11937	−0.10617	−0.09183
4d	−0.13172	−0.11937	−0.10617	−0.09183
n (4d)	0.6535	0.9847	1.2956	1.5896

Atom	Rh	Pd	Ag	Cd	In
Z	45	46	47	48	49
1s	−820.927173	−860.048546	−900.232540	−941.381019	−983.552576
2s	−116.614569	−123.041777	−129.790427	−136.759252	−144.005647
2p	−108.163817	−114.343011	−120.842024	−127.559951	−134.554225
3s	−20.585170	−22.008434	−23.620128	−25.317963	−27.159345
3p	−17.234646	−18.528092	−20.009041	−21.575259	−23.284171
3d	−11.035987	−12.079263	−13.308869	−14.622541	−16.077676
4s	−2.661143	−2.845456	−3.173860	−3.543470	−4.010922
4p	−1.645733	−1.771555	−2.037653	−2.343065	−2.744597
4d	−0.103288	−0.118970	−0.252103	−0.420723	−0.681578
5s			−0.124136	−0.167825	−0.253924
5p					−0.071162

Atom	Sn	Sb	Te	I	Xe
Z	50	51	52	53	54
1s	−1026.665599	−1070.725180	−1115.731902	−1161.685673	−1208.586286
2s	−151.449408	−159.095276	−166.943588	−174.994060	−183.246330
2p	−141.744613	−149.135914	−156.728514	−164.522166	−172.516543
3s	−29.062993	−31.033521	−33.071174	−35.175601	−37.346393
3p	−25.054553	−26.891049	−28.793930	−30.762871	−32.797483
3d	−17.593291	−19.174056	−20.820270	−22.531629	−24.307764
4s	−4.493043	−4.994724	−5.516439	−6.058048	−6.619330
4p	−3.159222	−3.592188	−4.044198	−4.515264	−5.005277
4d	−0.954355	−1.244953	−1.554330	−1.882595	−2.229668
5s	−0.330583	−0.404626	−0.477952	−0.551382	−0.625352
5p	−0.110212	−0.148390	−0.186783	−0.225814	−0.265689

Appendix C: Accidental degeneracies and nonuniqueness of the rHF ground state density matrix

When the Fermi level is negative and contains a pair of accidentally degenerate s and d shells, any nonmagnetic rHF ground state density matrix is of the form

$$\gamma_{Z,Z}^{0,\mathrm{rHF}} = 2\mathbb{1}_{(-\infty,\epsilon_{Z,Z,\mathrm{F}}^{0,\mathrm{rHF}})}(H_{Z,Z}^{0,\mathrm{rHF}}) + \alpha|\phi_s\rangle\langle\phi_s| + \sum_{m,m'=-2}^{2} \beta_{m,m'}|\phi_{d,m}\rangle\langle\phi_{d,m'}| + \sum_{m=-2}^{2} \gamma_m(|\phi_s\rangle\langle\phi_{d,m}| + |\phi_{d,m}\rangle\langle\phi_s|),$$

where $\alpha \in \mathbb{R}$, $\beta \in \mathbb{R}_{\mathrm{sym}}^{5\times 5}$ and $\gamma \in \mathbb{R}^5$ are matrices such that $0 \le \left(\begin{smallmatrix} \alpha & \gamma^T \\ \gamma & \beta \end{smallmatrix}\right) \le 2$, and

$$\phi_s(\boldsymbol{r}) = f_{ns}(r), \quad \phi_{d,m}(\boldsymbol{r}) = r^2 f_{n'd}(r)\widetilde{Y}_2^m(\theta,\varphi).$$

Here, the $\widetilde{Y}_l^m$ are the real spherical harmonics, and f_{ns} and $f_{n'd}$ are radial functions with $(n-1)$ and $(n'-3)$ nodes in $(0,+\infty)$, respectively. Since all the ground state density matrices share the same density, the function

$$\begin{aligned}\alpha^2 f_{ns}(r)^2 + \frac{\sqrt{15}}{\pi} f_{ns}(r) f_{n'd}(r)\Bigg(\gamma_{-2}xy + \gamma_{-1}yz + \gamma_0 \frac{2z^2-x^2-y^2}{\sqrt{3}} \\ + \gamma_1 xz + \gamma_2 \frac{x^2-y^2}{2}\Bigg) \\ + \frac{15}{4\pi} f_{n'd}(r)^2 \Bigg(\beta_{-2,-2}x^2y^2 + \beta_{-1,-1}y^2z^2 + \beta_{0,0}\frac{(2z^2-x^2-y^2)^2}{\sqrt{3}} + \beta_{1,1}x^2z^2 \\ + \beta_{2,2}\frac{(x^2-y^2)^2}{4} + 2\beta_{-2,-1}xy^2z + \beta_{-2,0}\frac{xy(2z^2-x^2-y^2)}{\sqrt{3}} \\ + 2\beta_{-2,1}x^2yz + \beta_{-2,2}xy(x^2-y^2) + \beta_{-1,0}\frac{yz(2z^2-x^2-y^2)}{12} \\ + 2\beta_{-1,1}xyz^2 + \beta_{-1,2}yz(x^2-y^2) + \beta_{0,1}\frac{xz(2z^2-x^2-y^2)}{\sqrt{3}} \\ + \beta_{0,2}\frac{(x^2-y^2)(2z^2-x^2-y^2)}{2\sqrt{3}} + \beta_{1,2}xz(x^2-y^2)\Bigg)\end{aligned}$$

where $r=(x^2+y^2+z^2)^{1/2}$, must be a function of r, independent of the chosen ground state density matrix. Since f_{ns} has more nodes than $f_{n'd}$ (we have seen above that $n=5$ or 6 and $n'=3$ or 4), this implies that β is a scalar matrix, that $\gamma=0$, and that only one value for the pair (α,β) is possible. This demonstrates the uniqueness of the nonmagnetic ground state when the Fermi level is negative and contains a pair of accidentally degenerate s and d shells.

When the Fermi level is negative and contains a pair of accidentally degenerate p and d shells, any nonmagnetic ground state density matrix is of the form

$$\begin{aligned}\gamma_{Z,Z}^{0,\mathrm{rHF}} = 2\mathbb{1}_{(-\infty,\epsilon_{Z,Z,\mathrm{F}}^{0,\mathrm{rHF}})}(H_{Z,Z}^{0,\mathrm{rHF}}) + \sum_{m,m'=-1}^{1} \alpha_{m,m'}|\phi_{p,m}\rangle\langle\phi_{p,m'}| \\ + \sum_{m,m'=-2}^{2} \beta_{m,m'}|\phi_{d,m}\rangle\langle\phi_{d,m'}| + \sum_{m=-1}^{1}\sum_{m'=-2}^{2} \gamma_{m,m'}(|\phi_{p,m}\rangle\langle\phi_{d,m'}| + |\phi_{d,m'}\rangle\langle\phi_{p,m}|) \qquad (59)\end{aligned}$$

where $\alpha \in \mathbb{R}^{3\times3}_{\mathrm{sym}}$, $\beta \in \mathbb{R}^{5\times5}_{\mathrm{sym}}$ and $\gamma \in \mathbb{R}^{3\times5}$ are matrices such that $0 \le \left(\begin{smallmatrix}\alpha & \gamma \\ \gamma^T & \beta\end{smallmatrix}\right) \le 2$, and

$$\phi_{p,m}(\boldsymbol{r}) = r f_{np}(r)\widetilde{Y}_1^m(\theta,\phi), \qquad \phi_{d,m}(\boldsymbol{r}) = r^2 f_{n'd}(r)\widetilde{Y}_2^m(\theta,\varphi).$$

Here, f_{np} and $f_{n'd}$ are radial functions with $(n-2)$ and $(n'-3)$ nodes in $(0,+\infty)$, respectively. Since all the ground state density matrices share the same density, the

function

$$
\begin{aligned}
&\frac{3}{4\pi} f_{np}(r)^2(\alpha_{-1,-1}y^2+\alpha_{0,0}z^2+\alpha_{1,1}x^2+2\alpha_{-1,0}yz+2\alpha_{-1,1}xy+2\alpha_{0,1}xz)\\
&+\frac{3\sqrt{5}}{2\pi} f_{np}(r)f_{n'd}(r)\Bigg(\gamma_{-1,-2}xy^2+\gamma_{-1,-1}y^2z+\gamma_{-1,0}\frac{y(2z^2-x^2-y^2)}{2\sqrt{3}}\\
&\qquad+\gamma_{-1,1}xyz+\gamma_{-1,2}\frac{y(x^2-y^2)}{2}+\gamma_{0,-2}xyz+\gamma_{0,-1}yz^2\\
&\qquad+\gamma_{0,0}\frac{z(2z^2-x^2-y^2)}{2\sqrt{3}}+\gamma_{0,1}xz^2+\gamma_{0,2}\frac{z(x^2-y^2)}{2}+\gamma_{1,-2}x^2y\\
&\qquad+\gamma_{1,-1}xyz+\gamma_{1,0}\frac{x(2z^2-x^2-y^2)}{2\sqrt{3}}+\gamma_{1,1}x^2z+\gamma_{1,2}\frac{x(x^2-y^2)}{2}\Bigg)\\
&+\frac{15}{4\pi} f_{n'd}(r)^2\Bigg(\beta_{-2,-2}x^2y^2+\beta_{-1,-1}y^2z^2+\beta_{0,0}\frac{(2z^2-x^2-y^2)^2}{12}\\
&\qquad+\beta_{1,1}x^2z^2+\beta_{2,2}\frac{(x^2-y^2)^2}{4}+2\beta_{-2,-1}xy^2z+\beta_{-2,0}\frac{xy(2z^2-x^2-y^2)}{\sqrt{3}}\\
&\qquad+2\beta_{-2,1}x^2yz+\beta_{-2,2}xy(x^2-y^2)+\beta_{-1,0}\frac{yz(2z^2-x^2-y^2)}{\sqrt{3}}\\
&\qquad+2\beta_{-1,1}xyz^2+\beta_{-1,2}yz(x^2-y^2)+\beta_{0,1}\frac{xz(2z^2-x^2-y^2)}{\sqrt{3}}\\
&\qquad+\beta_{0,2}\frac{(x^2-y^2)(2z^2-x^2-y^2)}{2\sqrt{3}}+\beta_{1,2}xz(x^2-y^2)\Bigg),
\end{aligned}
$$

where $r=(x^2+y^2+z^2)^{1/2}$, must be a function of r, independent of the chosen ground state density matrix. Since f_{np} has more nodes than $f_{n'd}$, this implies that α and β are scalar matrices and that, for α and β given, the function

$$
\begin{aligned}
&\gamma_{-1,-2}xy^2+\gamma_{-1,-1}y^2z+\gamma_{-1,0}\frac{y(2z^2-x^2-y^2)}{2\sqrt{3}}+\gamma_{-1,1}xyz+\gamma_{-1,2}\frac{y(x^2-y^2)}{2}\\
&\qquad+\gamma_{0,-2}xyz+\gamma_{0,-1}yz^2+\gamma_{0,0}\frac{z(2z^2-x^2-y^2)}{2\sqrt{3}}+\gamma_{0,1}xz^2+\gamma_{0,2}\frac{z(x^2-y^2)}{2}\\
&\qquad+\gamma_{1,-2}x^2y+\gamma_{1,-1}xyz+\gamma_{1,0}\frac{x(2z^2-x^2-y^2)}{2\sqrt{3}}+\gamma_{1,1}x^2z+\gamma_{1,2}\frac{x(x^2-y^2)}{2}
\end{aligned}
$$

is a given function of r. The vector space of homogeneous polynomials in x, y, z of total degree equal to 3 is of dimension 10, and the matrix γ has 15 independent entries. Provided α and β are not equal to 0 (which is suggested by our numerical simulations), an infinity of density matrices of the form (59) satisfy the rHF equations, and are therefore admissible nonmagnetic ground states.

Acknowledgements

The authors are grateful to Carlos García-Cervera and Vikram Gavini for valuable discussions.

References

[1] A. Anantharaman and E. Cancès, *Existence of minimizers for Kohn–Sham models in quantum chemistry*, Ann. Inst. H. Poincaré Anal. Non Linéaire **26** (2009), no. 6, 2425–2455. MR Zbl

[2] H. A. Bethe and E. E. Salpeter, *Quantum mechanics of one- and two-electron atoms*, Springer, 1957. MR Zbl

[3] E. Cancès, A. Deleurence, and M. Lewin, *A new approach to the modeling of local defects in crystals: the reduced Hartree–Fock case*, Comm. Math. Phys. **281** (2008), no. 1, 129–177. MR Zbl

[4] E. Cancès, S. Lahbabi, and M. Lewin, *Mean-field models for disordered crystals*, J. Math. Pures Appl. (9) **100** (2013), no. 2, 241–274. MR Zbl

[5] E. Cancès and C. Le Bris, *Can we outperform the DIIS approach for electronic structure calculations?*, Int. J. Quantum Chem. **79** (2000), no. 2, 82–90.

[6] E. Cancès and C. Le Bris, *On the convergence of SCF algorithms for the Hartree–Fock equations*, M2AN Math. Model. Numer. Anal. **34** (2000), no. 4, 749–774. MR Zbl

[7] E. Cancès and N. Mourad, *A mathematical perspective on density functional perturbation theory*, Nonlinearity **27** (2014), no. 9, 1999–2033. MR Zbl

[8] ———, *Existence of a type of optimal norm-conserving pseudopotentials for Kohn–Sham models*, Commun. Math. Sci. **14** (2016), no. 5, 1315–1352. MR Zbl

[9] ———, *A numerical study of the extended Kohn–Sham ground states of atoms*, preprint, 2017. arXiv

[10] I. Catto, C. Le Bris, and P.-L. Lions, *On the thermodynamic limit for Hartree–Fock type models*, Ann. Inst. H. Poincaré Anal. Non Linéaire **18** (2001), no. 6, 687–760. MR Zbl

[11] E. U. Condon and H. Odabaşı, *Atomic structure*, Cambridge University, 1980.

[12] P. A. M. Dirac, *Quantum mechanics of many-electron systems*, P. Roy. Soc. Lond. A **123** (1929), no. 792, 714–733. Zbl

[13] R. M. Dreizler and E. K. U. Gross, *Density functional theory: an approach to the quantum many-body problem*, Springer, 1990. Zbl

[14] C. Fefferman and L. A. Seco, *On the Dirac and Schwinger corrections to the ground-state energy of an atom*, Adv. Math. **107** (1994), no. 1, 1–185. MR Zbl

[15] G. Friesecke and B. D. Goddard, *Explicit large nuclear charge limit of electronic ground states for Li, Be, B, C, N, O, F, Ne and basic aspects of the periodic table*, SIAM J. Math. Anal. **41** (2009), no. 2, 631–664. MR Zbl

[16] C. Froese Fischer, *The Hartree–Fock method for atoms: a numerical approach*, Wiley, 1977.

[17] C. Froese Fischer, T. Brage, and P. Jönsson, *Computational atomic structure: an MCHF approach*, Institute of Physics, 1997. Zbl

[18] D. Gontier, *N-representability in noncollinear spin-polarized density-functional theory*, Phys. Rev. Lett. **111** (2013), no. 15, 153001.

[19] M. Hoffmann-Ostenhof and T. Hoffmann-Ostenhof, *"Schrödinger inequalities" and asymptotic behavior of the electron density of atoms and molecules*, Phys. Rev. A (3) **16** (1977), no. 5, 1782–1785. MR

[20] W. Kohn and L. J. Sham, *Self-consistent equations including exchange and correlation effects*, Phys. Rev. (2) **140** (1965), A1133–A1138. MR

[21] V. Korobov and A. Yelkhovsky, *Ionization potential of the helium atom*, Phys. Rev. Lett. **87** (2001), no. 19, 193003.

[22] E. S. Kryachko and E. V. Ludeña, *Density functional theory: foundations reviewed*, Phys. Rep. **544** (2014), no. 2, 123–239. MR

[23] M. Levy, *Universal variational functionals of electron densities, first-order density matrices, and natural spin-orbitals and solution of the v-representability problem*, Proc. Nat. Acad. Sci. U.S.A. **76** (1979), no. 12, 6062–6065. MR

[24] E. H. Lieb, *Density functionals for Coulomb systems*, Int. J. Quantum Chem. **24** (1983), no. 3, 243–277.

[25] E. H. Lieb and B. Simon, *The Hartree–Fock theory for Coulomb systems*, Comm. Math. Phys. **53** (1977), no. 3, 185–194. MR

[26] M. G. Medvedev, I. S. Bushmarinov, J. Sun, J. P. Perdew, and K. A. Lyssenko, *Density functional theory is straying from the path toward the exact functional*, Science **355** (2017), no. 6320, 49–52.

[27] N. Mourad, *Numerical computation of the extended Kohn–Sham ground states of atoms for cylindrically symmetric systems*, source code, 2017, version 1.0.

[28] R. G. Parr and Y. Weitao, *Density-functional theory of atoms and molecules*, International Series of Monographs on Chemistry, no. 16, Oxford University, 1989.

[29] J. P. Perdewk and A. Zunger, *Self-interaction correction to density-functional approximations for many-electron systems*, Phys. Rev. B **23** (1981), no. 10, 5048–5079.

[30] W. H. Press, S. A. Teukolsky, W. T. Vetterling, and B. P. Flannery, *Numerical recipes in FORTRAN: the art of scientific computing*, 2nd ed., Cambridge University, 1992. MR Zbl

[31] M. Reed and B. Simon, *Methods of modern mathematical physics*, vol. IV: Analysis of operators, Academic, 1978. MR Zbl

[32] M. E. Rose, *Elementary theory of angular momentum*, Wiley, 1957. MR Zbl

[33] H. Siedentop and R. Weikard, *On the leading energy correction for the statistical model of the atom: interacting case*, Comm. Math. Phys. **112** (1987), no. 3, 471–490. MR Zbl

[34] J. C. Slater, *A simplification of the Hartree–Fock method*, Phys. Rev. **81** (1951), no. 3, 385–390. Zbl

[35] J. P. Solovej, *Proof of the ionization conjecture in a reduced Hartree–Fock model*, Invent. Math. **104** (1991), no. 2, 291–311. MR Zbl

[36] J. P. Solovej, T. O. Sørensen, and W. L. Spitzer, *Relativistic Scott correction for atoms and molecules*, Comm. Pure Appl. Math. **63** (2010), no. 1, 39–118. MR Zbl

[37] A. H. Stroud and D. Secrest, *Gaussian quadrature formulas*, Prentice-Hall, 1966. MR Zbl

[38] L. Szasz, *The electronic structure of atoms*, Wiley, 1992.

[39] M. Trsic and A. B. da Silva, *Electronic, atomic and molecular calculations: applying the generator coordinate method*, Elsevier, 2007.

[40] S. M. Valone, *Consequences of extending* 1 *matrix energy functionals from pure-state representable to all ensemble representable* 1 *matrices*, J. Chem. Phys. **73** (1980), no. 3, 1344–1349. MR

Received February 7, 2017. Revised February 25, 2018.

ERIC CANCÈS: eric.cances@enpc.fr
Centre d'Enseignement et de Recherche en Mathématiques et Calcul Scientifique, Ecole des Ponts ParisTech and Institut National de Recherche en Informatique et en Automatique Paris, Université Paris-Est, Marne-la-Vallée, France

NAHIA MOURAD: nahia.mourad@gmail.com
Centre d'Enseignement et de Recherche en Mathématiques et Calcul Scientifique, Ecole des Ponts ParisTech, Université Paris-Est, Marne-la-Vallée, France

mathematical sciences publishers msp

Communications in Applied Mathematics and Computational Science

msp.org/camcos

EDITORS

MANAGING EDITOR

John B. Bell
Lawrence Berkeley National Laboratory, USA
jbbell@lbl.gov

BOARD OF EDITORS

Marsha Berger	New York University berger@cs.nyu.edu
Alexandre Chorin	University of California, Berkeley, USA chorin@math.berkeley.edu
Phil Colella	Lawrence Berkeley Nat. Lab., USA pcolella@lbl.gov
Peter Constantin	University of Chicago, USA const@cs.uchicago.edu
Maksymilian Dryja	Warsaw University, Poland maksymilian.dryja@acn.waw.pl
M. Gregory Forest	University of North Carolina, USA forest@amath.unc.edu
Leslie Greengard	New York University, USA greengard@cims.nyu.edu
Rupert Klein	Freie Universität Berlin, Germany rupert.klein@pik-potsdam.de
Nigel Goldenfeld	University of Illinois, USA nigel@uiuc.edu
Ahmed Ghoniem	Massachusetts Inst. of Technology, USA ghoniem@mit.edu
Raz Kupferman	The Hebrew University, Israel raz@math.huji.ac.il
Randall J. LeVeque	University of Washington, USA rjl@amath.washington.edu
Mitchell Luskin	University of Minnesota, USA luskin@umn.edu
Yvon Maday	Université Pierre et Marie Curie, France maday@ann.jussieu.fr
James Sethian	University of California, Berkeley, USA sethian@math.berkeley.edu
Juan Luis Vázquez	Universidad Autónoma de Madrid, Spain juanluis.vazquez@uam.es
Alfio Quarteroni	Ecole Polytech. Féd. Lausanne, Switzerland alfio.quarteroni@epfl.ch
Eitan Tadmor	University of Maryland, USA etadmor@cscamm.umd.edu
Denis Talay	INRIA, France denis.talay@inria.fr

PRODUCTION

production@msp.org

Silvio Levy, Scientific Editor

See inside back cover or msp.org/camcos for submission instructions.

The subscription price for 2018 is US $100/year for the electronic version, and $150/year (+$15, if shipping outside the US) for print and electronic. Subscriptions, requests for back issues from the last three years and changes of subscriber address should be sent to MSP.

Communications in Applied Mathematics and Computational Science (ISSN 2157-5452 electronic, 1559-3940 printed) at Mathematical Sciences Publishers, 798 Evans Hall #3840, c/o University of California, Berkeley, CA 94720-3840, is published continuously online. Periodical rate postage paid at Berkeley, CA 94704, and additional mailing offices.

CAMCoS peer review and production are managed by EditFLOW® from MSP.

PUBLISHED BY

mathematical sciences publishers

nonprofit scientific publishing

http://msp.org/

© 2018 Mathematical Sciences Publishers

Communications in Applied Mathematics and Computational Science

vol. 13 no. 2 2018

A numerical study of the extended Kohn–Sham ground states of atoms 139
Eric Cancès and Nahia Mourad

An equation-by-equation method for solving the multidimensional moment constrained maximum entropy problem 189
Wenrui Hao and John Harlim

Symmetrized importance samplers for stochastic differential equations 215
Andrew Leach, Kevin K. Lin and Matthias Morzfeld

Efficient high-order discontinuous Galerkin computations of low Mach number flows 243
Jonas Zeifang, Klaus Kaiser, Andrea Beck, Jochen Schütz and Claus-Dieter Munz

A numerical study of the relativistic Burgers and Euler equations on a Schwarzschild black hole exterior 271
Philippe G. LeFloch and Shuyang Xiang

A semi-implicit multiscale scheme for shallow water flows at low Froude number 303
Stefan Vater and Rupert Klein

1559-3940(2018)13:2;1-B